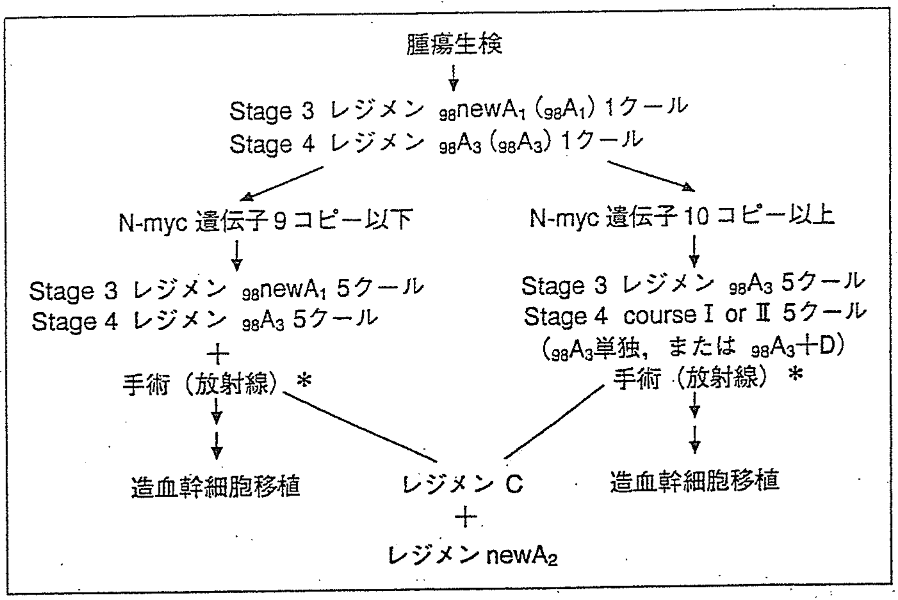

図1．治療法のフローチャート
＊：手術(放射線)は $_{98}A_3$ など，初期6クールのいずれかの時期に施行する．

で16例が治療関連死である[11]．またN-mycの増幅に関しても検索した1,197例中10コピー以上の増幅例は11例のみであり，予後因子も良好である[11]．現在N-mycの増幅などの悪性度の高い症例を除き，マス症例に対してより縮小した外科的治療，化学療法を行っており[12]，われわれは腹腔鏡下腫瘍摘出術などの縮小手術を施行している[13]．また，施設によっては一定の基準を設けて経過観察を行っており，61%の症例に腫瘍の消失または縮小を認めている[14]．日本小児がん学会神経芽腫委員会によるretrospective cohort studyではマススクリーニングは1歳以上の神経芽腫発生率は減少させておらず，有効性は明らかでなかった[15]．厚生労働省は2003年7月にマススクリーニングの意義が明らかでないため，一応休止する報告書が出された。

この10年間に多くの神経芽腫の予後因子に関する研究が行われてきている[16]．その結果を簡単にまとめると，予後不良因子としてN-myc癌遺伝子の増幅[17]，染色体1pの欠失[16]，DNA核型がdiploidy[18]，血管新生因子であるVEGF発現[19]，アポトーシスを抑制するsurvivin遺伝子の発現[20]などが明らかとなった．一方，予後良好な因子として，癌遺伝子であるHa-rasの遺伝子産物であるp21の発現[21]，細胞接着分子であるCD44の発現[22]，nerve growth factorのレセプターであるTrk-Aの発現[16]が明らかとなった．これらの予後良好因子はマススクリーニングで発見された予後良好である症例に発現が認められることより，腫瘍が分化しアポトーシスにいたるためであると推察される[16]．最近の研究により癌抑制遺伝子が1p36に存在することがかなり濃厚となってきた[23]．マススクリーニング症例の生存率は98%と予後良好であるが，その発生に関して癌抑制遺伝子がどのように関与しているかが今後明らかになってくるのではないかと期待される．

II．腎芽腫(Wilms腫瘍)

Wilms腫瘍は神経芽腫に次いで多い小児悪性固形腫瘍である[2]．年間発生頻度は100例前後と推察される．発見時年齢は乳児期より1歳の頻度が高く，90%以上は5歳以下に発見されている．

本腫瘍は後腎(metanephric blastema)から発生すると考えられており，大部分は片側性であるが5～10%が両側性に発生する．また，本腫瘍は無虹彩症(aniridia)，片側肥大(hemihypertrophy)，

表2. 日本Wilms腫瘍スタディグループの治療方針

病期，組織分類	放射線	化学療法	投与期間
病期I，II，FH	なし	EE-4A	18週
病期I，focal or diffuse anaplasia	なし	EE-4A	18週
病期III，IV，FHおよび病期II-IV，focal anaplasia	1,080 cGy	DD-4A	24週
病期II-IV，diffuse anaplasiaおよびCCSK	1,080 cGy	I	24週
病期I，II，RTK	なし	RTK	24週
病期III，IV，RTK	1,080 cGy	RTK	24週

EMG症候群(Beckwith-Wiedemann症候群)を合併することがある．最近の研究により，これらの症例に11番染色体の短腕の欠損が報告されており，さらに癌抑制遺伝子WT1が発見され，本腫瘍の発生に強く関与していることが明らかになっている[24]．また，本腫瘍は血行性に肺転移をきたしやすいことが特徴である．

本腫瘍の治療成績は1969年に開始された米国のNational Wilms Tumor Study(NWTS)で化学療法としてactinomycin-D(AMD)および放射線療法の導入によりその治療成績は著しく改善した[25,26]．そして，本来の腎芽腫は化学療法により予後良好(favorable type：FH)であるのに対し，unfavorable type(UH)としてanaplasiaを伴うanaplastic subtypeは予後不良であり，さらにそれらと明らかに組織型が異なるmalignant rhabdoid tumor of the kidney(MRTK)，clear cell sarcoma of the kidney(CCSK)も予後不良であることが明らかとなった．NWTS-3(1979～1985年)の成績では，病期IIIおよびUF症例にadriamycin(ADR)を導入することにより全体の2年生存率は90%に向上している[27]．

病期別では，FHのI期(2年生存率90%)，II期(2年生存率90%)と予後良好で，化学療法はvincristine sulfate(VCR)＋AMDのみ(レジメンEE)で，放射線療法は省略できることが明らかとなった．FHのIII期(2年生存率85%)，IV期(2年生存率80%)も予後良好で，VCR＋AMD＋ADR(レジメンDD)の化学療法と1,080 cGyの放射線療法で十分で，cyclophosphamide(CPM)を加える必要がないことが明らかとなった．FHのV期(両側性)も2年生存率は87%と良好であった．UHのI～III期(2年生存率70%)，IV期(2年生存率58%)の予後はCPMを加えたVCR＋AMD＋ADR＋CPMの化学療法＋放射線療法で改善している[28]．

NWTS-4は1986年より1994年に施行され，NWTS-3では5日間投与のAMDおよび3日間投与のADRの投与を1日の静注に変更して，治療効果を維持しながら入院期間および副作用の軽減を図ろうとした．その結果，low risk patient(I-II期，FH，I期anaplasia)の2年無再発生存率(2年RFS)91%，high risk patient(III-IV期FH)の2年RFS 90%と良好であり，骨髄抑制も少なく，入院期間の短縮が可能になった[29]．

また，anaplasiaをfocal anaplasiaとdiffuse anaplasiaに新分類し，focal anaplasiaの4年RFSは80%以上であるのに対し，diffuse anaplasiaの4年RFSは50%以下と，diffuse anaplasiaは予後が不良であることが明らかとなった[30]．Stage Iに関しては，focalとdiffuseは生存率に差がなく予後良好である．以上の治療成績をふまえて，NWTS-5ではUHのうちでII期以上のdiffuse anaplasiaに対してレジメンI(VCR＋ADR＋VP-16＋CPM)が開始され，本邦でも1996年よりNWTS-5に則ったプロトコルで全国的なグループスタディが開始されている(表2)[31]．CCSKは比較的まれな組織型を呈する腎腫瘍で，骨，脳，軟部組織への転移をきたしやすくFHに比べ予後不良である．NWTS-3にてVCR，AMDにADRを加えることで2年RFSは68%に改善している[27]．NWTS-5ではレジメンIの治療が行われて

表3. 化学療法(JPLT-2プロトコル)

プロトコル名 low-CITA			
day 1	CDDP	40 mg/m²/日	24時間 静注
day 2	THP-ADR	30 mg/m²/日	1時間 静注
プロトコル名 CITA			
day 1	CDDP	80 mg/m²/日	24時間 静注
day 2, 3	THP-ADR	30 mg/m²/日×2	1時間 静注 (計60 mg)
プロトコル名 CITA-L (TACE)			
	carboplatin (200 mg/m²)		
	THP-ADR (30 mg/m²)+リピオドール		
	slow transarterial injection		
プロトコル名 ITEC			
day 1, 2	IFO	3.0 g/m²/日×2	2時間 静注 (計6.0 g)
day 3	carboplatin	400 mg/m²/日	24時間 静注
day 4, 5	THP-ADR	30 mg/m²/日×2	1時間 静注 (計60 mg)
day 1, 2, 3, 4, 5	etoposide (VP16)	100 mg/m²/日×5	1時間 静注 (計500 mg)

いる.

MRTKは1歳以下の乳児に多くみられ，その予後はきわめて不良である．また，未分化神経外胚葉性腫瘍(PNET)などの中枢神経腫瘍の合併が10%みられる．NWTS-3ではレジメンDDとレジメンJのあいだで比較が行われたが，4年RFSはそれぞれ23.1%，26.7%と不良であった．NWTS-5ではレジメンRTK(CPM+VP16+carboplatin)が試みられている．これまでの日本Wilms腫瘍スタディ(JWiTS)の成績では依然予後不良であり，さらに強力な治療法の導入が必要と考えられる．

また予後不良因子として，16q，1pのloss of heterozygosity(LOH)が再発率，死亡率が高いことが報告され，腫瘍増殖や転移能などに関する遺伝子の存在が疑われる．NWTS-5でのpreliminary resultsでは，それぞれのLOHと予後との相関はみられないが，1pと16qがともにLOHである症例は予後不良である結果が得られている．今後，予後因子として治療の層別化に有用である可能性がある[32~35]．また，術前化学療法についてはヨーロッパを中心としたInternational Society of Pediatric Oncology(SIOP)のスタディ[36]が行われているが，その適応として，摘出不能症例，下大静脈内伸展症例，bilateral tumorがあげられる．下大静脈内伸展症例は術前化学療法により手術の合併症を防ぐことができるし，bilateral tumorでは両側腎を部分切除のみで温存できる可能性がある[37]．また，aniridia，Beckwith-Wiedemann症候群で経過観察中に発見した症例も，将来反対側に腫瘍が発生する可能性があるので腎部分切除を心がける必要がある．

III. 肝芽腫(hepatoblastoma)

小児肝癌の約80%を占める肝芽腫は，その根治療法は肝切除しかない[38]．以前は肝切除術がただちに施行されてきたが，肝切除が困難な症例も多く，術中・術後出血による死亡する症例も散見された．また肝芽腫は以前，化学療法が奏功しないとされていたが，CDDPおよびADRが有効であることが明らかとなり[39]，1991年より2区域以上を占める症例に対して，術前に化学療法を導入する日本独自のグループスタディ(JPLT)が開始された[40]．そのプロトコルは病期別にCDDP，pirarubicin hydrochloride(THP)-ADRの投与量，術前における化学療法および動注化学療法の有用性を中心に作成された．その結果，1991～1995年に103例の悪性腫瘍が登録され，うち95

例が肝芽腫であった．その結果，病期別2年生存率はI期100%，II期95.5%，IIIA期88.5%，IIIB期58.3%，IV期55.6%と治療成績は向上している[41]．われわれは1990年より術前肝動注化学療法および塞栓療法(TACE)を施行し，良好な治療成績を得ている[42]．TACEは原則として腫瘍の栄養動脈に選択的にカテーテルを挿入し，リピオドールに懸濁したTHP-ADRおよびCDDPを注入後，gelformにて塞栓術を施行する．TACE直後は短期間の発熱，CRPの上昇がみられたが，骨髄抑制は軽度であり腫瘍の縮小およびalpha-fetoprotein(AFP)値の低下がみられ，安全かつ早期に肝切除が可能であった．11例に施行したが，10例が無再発で生存中である．また，1999年11月より治療抵抗例や再発症例に対して幹細胞移植を併用した超大量療法化学療法を組みこんだJPLT-2プロトコルが開始された[43](表3)．われわれは肺転移症例に対して，早期よりの幹細胞移植を併用した超大量療法化学療法を施行後に肝切除，転移巣切除を行ってCRを得ており，その有効性が期待される[44]．また，肝芽腫におけるβカテニン異常が高率にあることが明らかになっている[45]．

おわりに

小児悪性固形腫瘍における治療成績の進歩の概略について述べた．10年以上前では予後不良であったこれらの腫瘍の治療成績は，グループスタディーによる集学的治療の導入により改善してきている．今後は分子生物学的解析により予後不良因子をより明確にし，それらの因子に基づいたrisk-based treatmentを導入することにより，小児癌患児のQOLの向上が期待される．

◆◆◆ 文献 ◆◆◆

1) Gurney JG, Severson RK, David S et al：Incidence of cancer in children in the United States. Cancer 75：2186-2190, 1995
2) 日本小児外科学会悪性腫瘍委員会：小児の外科的悪性腫瘍，2001年登録症例の全国集計結果の報告．日小児外会誌39：109-136，2003
3) Ikeda H, Suzuki N, Takahashi A et al：Surgical treatment of neuroblastomas in infants under 12 months of age. J Pediatr Surg 33：1246-1250, 1998
4) 日本小児外科学会悪性腫瘍委員会：小児悪性固形腫瘍5腫瘍の予後追跡調査結果の報告．日小児外会誌33：79-153，1997
5) 澤口重徳，金子道夫，中條俊夫ほか：統一治療プロトコールによる進行神経芽腫の治療．日小児外会誌26：121-127，1990
6) 福澤正洋，大植孝治，草深竹志ほか：自家骨髄移植を用いた進行神経芽腫治療における外科療法の意義．日小児外会誌32：877-883，1996
7) Kaneko M, Nishihira H, Mugishima H et al：Stratification of treatment of stage 4 neuroblastoma patients based on N-myc amplification status. Med Pediatr Oncol 31：1-7, 1998
8) Iwafuchi M, Utsumi J, Tsuchida Y et al：Evaluation of patients with advanced neuroblastoma surviving more than 5 years after initiation of an intensive Japanese protocol；a report from the study group of Japan for treatment of advanced neuroblastoma. Med Pediatr Oncol 27：515-520, 1996
9) Kaneko M, Tsuchida Y, Mugishima H et al：Intensified chemotherapy increases the survival rates in patients with stage 4 neuroblastoma with myc amplification. J Pediatr Hematol Ocol 24：613-621, 2002
10) Sawada T, Sugimoto T, Tanaka T et al：Number and cure rate of neuroblastoma cases detected by the mass screening program in Japan. Med Pediatr Oncol 15：14-17, 1987
11) 神経芽腫委員会：神経芽腫マス・スクリーニングの全国集計結果．小児がん40：286-298，1999
12) 福澤正洋，大植孝治，河本陽介ほか：神経芽腫マススクリーニング症例に対する治療法の検討．小児がん33：29-33，1996
13) Nakajima K, Fukuzawa M, Fukui Y et al：Laparoscopic resection of mass-screened adrenal neuroblastoma in an 8-month-old infant. Surg Laparosc Endosc 7：498-500, 1997
14) 神経芽腫委員会：マススクリーニングで発見され無治療で経過観察された神経芽腫82例．小児がん39：131-136，2002
15) 水田祥代，澤田　淳，金子道夫ほか：平成10年日本小児がん学会神経芽腫委員会報告．小児

がん 36：107-117, 1999
16) Brodeur GM, Nakagawara A：Molecular basis of clinical heterogeneity in neuroblastoma. Am J Pediatr Hematol Oncol 14：111-116, 1992
17) Seeger RC, Brodeur GM, Sather H et al：Association of multiple copies of neuroblastomas. N Engl J Med 313：111-116, 1985
18) Kusafuka T, Nagahara N, Oue T et al：Unfavorable DNA ploidy and Ha-ras p21 findings in neuroblastoma detected through mass screening. Cancer 76：695-699, 1995
19) Fukuzawa M, Sugiura H, Koshinaga T et al：Expression of vascular endothelial factor and its receptor Flk-1 in human neuroblastoma using *in situ* hybridization. J Pediatr Surg 37：1747-1750, 2002
20) Azuhata T, Scott D, Takamizawa S et al：The inhibitor of apoptosis protein surviving is associated with high-risk behavor of neuroblastoma. J Pediatr Surg 37：1747-1750, 2002
21) Tanaka T, Sugimoto T, Sawada T：Prognostic discrimination amang neuroblastomas according to Ha-ras/trk A gene expression. Cancer 83：1626-1633, 1998
22) Comito MA, Savell VH, Cohen MB：CD44 expression in neuroblastoma and related tumors. J Pediatr Hematol Oncol 19：292-296, 1997
23) Altura RA, Maris JM, Li H et al：Novel regions of chromosomal loss in familial neuroblastoma by comparative genomic hybridization. Genes Chromosom Cancer 19：176-184, 1997
24) Call KM, Glaser T, Ito CY et al：Isolation and characterization of a zinc finger polypeptide gene at the human chromosome 11 Wilms' tumor locus. Cell 60：509-520, 1990
25) D'Angio GJ, Evans AE, Breslow N et al：The treatment of Wilms' tumor；results of the national Wilms' tumor study. Cancer 38：633-646, 1976
26) D'Angio GJ, Evans AE, Breslow N et al：The treatment of Wilms' tumor；results of the second national Wilms' tumor study. Cancer 47：2302-2311, 1981
27) D'Angio GJ, Breslow N, Beckwith B et al：Treatment of Wilms' tumor, results of the third national Wilms' tumor study. Cancer 64：349-360, 1989
28) Levien MG, Bringelsen KA：Postoperative chemotherapy in the national Wilms' tumor studies. Semin Urol Oncol 17：40-45, 1999
29) Green DM, Norman EB, Evans I et al：The effect of chemotherapy dose intensity on the hematological toxicity of the treatment for Wilms' tumor. Am J Pediatr Hematol Oncol 16：207-212, 1994
30) Green DM, Beckwith B, Breslow NE et al：Treatment of children with stages II to IV anaplastic Wilms' tumor；a report from the national Wilms' tumor study group. J Clin Oncol 12：2126-2131, 1994
31) 岩川真由実, 大川治夫, 大橋靖雄ほか：腎芽腫の病期・年齢による治療戦略と予後. 小児外科 34：1174-1179, 2002
32) Grundy PE, Telzerow PE, Breslow N et al：Loss of heterozygosity for chromosome 16q and 1p in Wilms' tumor predicts an adverse outcome. Cancer Res 54：2331-2333, 1994
33) Fong CT, White PS, PetersonJK et al：Loss of heterozygosity for chromosomes 1 and 14 defines subsets of advanced neuroblastomas. Cancer Res 52：1780-1785, 1992
34) Koufos A, Hansen MF, Lampkin BC et al：Loss of alleles of loci on human chromosome 11 during genesis of Wilms' tumor. Nature 309：170-172, 1984
35) Barrantes JC, Muir KR, Toyn CE et al：Thirty year population based review of childhood renal tumors with an assessment of prognostic factors including tumor DNA characteristics. Med Pediatr Oncol 21：24-30, 1993
36) Godzinski J, Tournade MF, Kraker JD et al：The role of preoperative chemotherapy in the treatment of nephroblastoma；the SIOP experience. Semin Urol Oncol 17：28-32, 1999
37) Ross JH, Kay R：Surgical consideration for Patients with Wilms' tumor. Semin Urol Oncol 17：33-39, 1999
38) Okada A, Fukuzawa M, Oue T et al：Thirty-eight years experience of malignant hepatic tumors in infants and childhood. Eur J Pediatr Surg 8：17-22, 1998
39) Godzinski J, Tournade MF, Kraker JD et al：

The role of preoperative chemotherapy in the treatment of nephroblastoma ; the SIOP experience. Semin Urol Oncol 17 : 28-32, 1999
40) 日本小児肝癌スタディグループ：グループスタディによる小児肝癌の治療―治療効果について．小児がん 31：367-371，1994
41) 日本小児肝癌スタディグループ：グループスタディによる小児肝癌の治療―治療成績について．小児がん 32：121-124，1995
42) Oue T, Fukuzawa M, Kusafuka T et al : Transcatheter arterial chemoembolization in the treatment of hepatoblastoma. J Pedia Surg 33 : 1771-1775, 1998
43) 大沼直躬，松永正訓，佐々木文章ほか：小児がんのグループスタディをめぐって―日本小児肝癌グループスタディ．小児外科 32：798-805 2000
44) 草深竹志，米田光宏，繆　江永ほか：両肺転移を伴う進行肝芽腫に対し集学的治療を施しCRを得た1治験例．小児がん 39：51-56，2002
45) 高安　肇：肝芽腫とβカテニン異常．小児外科 35：522-527，2003

お知らせ

◆第19回国際消化器外科会議

会　期：2004年12月8日(水)～11日(土)
会　場：パシフィコ横浜(横浜国際会議場)
会　長：嶋田　紘(横浜市立大学大学院医学研究科消化器病態外科学)
主　催：第19回国際消化器外科会議組織委員会
ISDS日本部会
後　援：文部科学省，厚生労働省，日本学術会議，神奈川県，横浜市
日本医師会，神奈川県医師会，横浜市医師会
SSAT，ISDE，SAGES，ASCRS他
日本消化器外科学会，日本外科学会，日本臨床外科学会，日本癌治療学会，
日本食道学会，日本肝胆膵外科学会，日本大腸肛門病学会，日本内視鏡外科学会
日本消化器病学会，日本消化器内視鏡外科学会，日本胆道学会，日本膵臓学会

今回の会議はメインテーマとして「21世紀のEBMとグローバルスタンダード」を，シンポジウム，パネルディスカッションのテーマとしては，各国の医学教育と医療制度の問題点，癌各種悪性度診断，食道癌の至適郭清，Barrett食道癌，センチネルナビゲーションサージャリー，EMR，ITメス，HCCの各種治療法，HCCに対する肝移植，CCCの病態に基づく治療法，肝門部肝胆癌の画像と局所解剖，胆嚢癌外科治療の限界，膵癌の早期発見，膵炎，大腸ポリープの扱い，直腸癌術式，肝肺転移の治療法などを予定しています．

学会主催事務局：〒236-0004 横浜市金沢区福浦3-9
横浜市立大学大学院医学研究科消化器病態外科学
担当：渡合伸治
TEL：045-787-2650/FAX：045-782-9161
E-mail：19isds@med.yokohama-cu.ac.jp
問い合せ先：〒100-0013 東京都千代田区霞が関1-4-2大同生命霞が関ビル18階
日本コンベンションサービス株式会社内
担当：加藤直樹
TEL：03-3508-1304/FAX：03-3508-1305
http：//www.19isds.com

Oncogene (2005) 24, 3385–3396

www.nature.com/onc

ORIGINAL PAPERS

topors, a p53 and topoisomerase I-binding RING finger protein, is a coactivator of p53 in growth suppression induced by DNA damage

Ling Lin[1,2,3], Toshinori Ozaki[4], Yuki Takada[1,2], Hajime Kageyama[4], Yoko Nakamura[4], Akira Hata[5], Jian-Hua Zhang[3], William F Simonds[3], Akira Nakagawara[4] and Haruhiko Koseki*[,1,2]

[1]*Department of Molecular Embryology, Graduate School of Medicine, Chiba University, 1-8-1 Inohana, Chuo-ku, Chiba 260-8670, Japan;* [2]*RIKEN Research Center for Allergy and Immunology, RIKEN Yokohama Institute, 1-7-22 Suehiro, Tsurumi-ku, Yokohama 230-0045, Japan;* [3]*Metabolic Diseases Branch, National Institute of Diabetes, Digestive and Kidney Diseases, NIH, Bethesda, MD 20892, USA;* [4]*Division of Biochemistry, Chiba Cancer Center Research Institute, 666-2 Nitona, Chuoh-ku, Chiba 260-8717, Japan;* [5]*Department of Public health, Graduate School of Medicine, Chiba University, 1-8-1 Inohana, Chuo-ku, Chiba 260-8670, Japan*

The RING family zinc-finger protein topors (topoisomerase I-binding protein) binds not only topoisomerase I, but also p53 and the AAV-2 Rep78/68 proteins. topors maps to human chromosome 9p21, which contains candidate tumor suppressor genes implicated in small cell lung cancers. In this study, we isolated the murine counterpart of topors and investigated its impact on p53 function. The deduced amino-acid sequence of mouse topors exhibits extensive similarity to human topors. Overexpressed myc-tagged topors associates with and stabilizes p53, and enhances the p53-dependent transcriptional activities of *p21^{Waf1}*, *MDM2* and *Bax* promoters and elevates endogenous *p21^{Waf1}* mRNA levels. Overexpression of topors consequently results in the suppression of cell growth by cell cycle arrest and/or by the induction of apoptosis. Taken together, these studies identify topors as a positive regulator of p53. The expression of *topors* is induced by exposure to the genotoxic reagents cisplatin and camptothecin, a DNA topoisomerase I inhibitor. We therefore postulate that topors mediates p53-dependent cellular responses induced by DNA damage, suggesting its physiological role as a tumor suppressor.
Oncogene (2005) **24,** 3385–3396. doi:10.1038/sj.onc.1208554
Published online 28 February 2005

Keywords: topors; p53; tumor suppressor; DNA damage; cell cycle; apoptosis

Introduction

The p53 tumor suppressor protein is defined as the guardian of the genome, and more than half of all human cancers are characterized by either the loss of the p53 protein or by mutations in its gene (Lane, 1992; Ko and Prives, 1996). The p53 protein comprises 393 amino acids including an amino-terminal transactivation domain, a sequence-specific DNA-binding domain and a multifunctional carboxyl-terminal domain. p53 is involved in the regulation of the cell cycle, apoptosis, senescence, DNA repair, cell differentiation and angiogenesis (Levine, 1997; Vogelstein *et al.*, 2000). These activities of p53 are mediated by one or more known mechanisms including the transcriptional regulation of target genes, functional regulation of interacting proteins, DNA annealing and exonuclease activity. p53 is activated by several stress conditions including DNA damage, the expression of several oncogene products, changes in cellular adhesion and redox potential, and reduction in the ribonucleoside triphosphate pool. In response to such stress signals, p53 undergoes extensive post-translational modification that modulates its stability and activity. The stabilization of p53 is presumed to play a major role in its activation, while modifications unrelated to p53 stabilization may regulate its specific activity (Sionov and Haupt, 1999; Vogelstein *et al.*, 2000). The stability of p53 is tightly regulated by multiple positive and negative feedback loops involving a number of p53 interacting proteins (Sionov and Haupt, 1999; Vogelstein *et al.*, 2000).

Human topoisomerase I-binding protein (h-topors) was first identified by yeast two-hybrid screening as a protein that interacts with human topoisomerase I (hTop1), and turned out to be identical to a novel p53-binding protein, p53BP3 (Haluska *et al.*, 1999; Zhou *et al.*, 1999). An identical protein was also isolated as the DNA-binding protein LUN, as a protein that interacts with adeno-associated virus type 2 (AAV-2) Rep78/68 proteins and as a protein binding to the interferon-inducible large GTPase Mx1 (Chu *et al.*, 2001; Engelhardt *et al.*, 2001; Weger *et al.*, 2002). h-topors is predicted to contain 1045 amino acids and to encode a RING family zinc-finger domain, a putative leucine zipper (LZ) domain, five sequences rich in proline, glutamine, serine and threonine (PEST sequences), an arginine/serine-rich (RS) domain and a bipartite nuclear localization signal (NLS). h-topors is

*Correspondence: H Koseki, RIKEN Research Center for Allergy and Immunology, RIKEN Yokohama Institute, 1-7-22 Suehiro, Tsurumi-ku, Yokohama 230-0045, Japan; E-mail: koseki@rcai.riken.jp
Received 1 June 2004; revised 18 January 2005; accepted 18 January 2005; published online 28 February 2005

modified by conjugation to the small ubiquitin-like modifier, SUMO-1 (Weger *et al.*, 2003), and both endogenous h-topors and overexpressed h-topors-GFP fusion protein are mainly distributed in promyelocytic leukemia-associated protein (PML) nuclear bodies in a PML protein-dependent fashion (Rasheed *et al.*, 2002). The carboxyl-terminal region of h-topors is required for such punctate nuclear localization (Rasheed *et al.*, 2002). In addition, the amino-terminal region of h-topors, containing the RING zinc-finger motif and LZ region, has been shown to bind to DNA in a sequence-specific as well as Zn^{2+}-dependent manner (Chu *et al.*, 2001). Since h-topors enhances the expression of a Rep78/68-dependent AAV-2 gene in the absence of helper virus, h-topors might be a transcriptional regulator (Weger *et al.*, 2002).

Although h-topors interacts with p53 as revealed by yeast two-hybrid assay, the role of h-topors in regulating the function of p53 remains to be clarified (Zhou *et al.*, 1999; Weger *et al.*, 2002). Several lines of evidence suggest that h-topors might be an important regulator in cell proliferation. Relocalization of topors in cells exposed to the Top1-targeting drug camptothecin (CPT) or the transcription inhibitor 5,6-dichloro-1-β-D-ribofuranolsylbenzimidazole (DRB) suggests its involvement in mediating the DNA damage response induced by CPT or DRB, which have been shown to cause an accumulation of p53 (Klibanov *et al.*, 2001; Rasheed *et al.*, 2002). h-topors interacts with AAV-2 Rep78, which has been proved to be an effective repressor of the adenovirus in the process of tumor generation (Schlehofer, 1994). Intriguingly, the region of h-topors required for interaction with AAV-2 Rep78/68 overlaps with that for p53 binding, as revealed by yeast two-hybrid analysis (Batchu *et al.*, 1999; Weger *et al.*, 2002). In addition, h-topors maps to chromosome 9p21, a locus containing candidate tumor suppressor gene(s) associated with the loss of heterozygosity in 86% of small cell lung cancers (Chu *et al.*, 2001). These observations prompted us to examine the functional role of topors in the regulation of p53. In the present study, we describe a physical and functional interaction between mouse topors and p53 in mammalian cultured cells. Our results strongly suggest that topors acts as a coactivator of p53 in response to DNA damage.

Results

Identification of a murine counterpart of topors

To identify proteins that interact with the Polycomb group (PcG) protein Mph2 (Yamaki *et al.*, 2002), we employed yeast-based two-hybrid screening using a cDNA library derived from mouse embryo and bait derived from full-length Mph2. We isolated two identical 1.2-kb cDNA fragments encoding a polypeptide highly homologous to the carboxyl-terminal half of h-topors. By conventional cDNA screening of a mouse brain cDNA library and database screening, two overlapping clones, a 3.5-kb fragment lacking the amino-terminal region and a mouse EST clone lacking the carboxyl-terminal region, were isolated. The nucleotide sequences of both clones were determined, and the combined nucleotide sequences revealed the longest open reading frame (ORF) of 1033 amino-acid residues with 86% overall identity to h-topors (DDBJ accession number: AB104865). In the amino-terminal region, a RING family zinc-finger domain and an LZ region exhibited 100 and 98% homology to h-topors, respectively (red letters and open blue box in Figure 1a, respectively). The p53-binding domains of h-topors were previously shown to be separated into two blocks based on yeast two-hybrid interactions (underlined in Figure 1a) (Zhou *et al.*, 1999; Weger *et al.*, 2002). A bipartite NLS was present in the amino-terminal block of the p53-binding domains (blue letters in Figure 1a). A cluster of residues including the two p53-binding subdomains and an intermediate region exhibited 90% identity with h-topors (Figure 1b). Because of the extensive similarity to h-topors, this newly isolated cDNA was identified as a murine counterpart of the *h-topors* gene. The mouse *topors* gene was mapped to a 40 Mb region of mouse chromosome 4 by BLAST analysis of the mouse genome (40017898–40007704 bp; Ensemble Mouse Genome Browser), a region syntenic to human chromosome 9p21. This chromosomal localization is in agreement with a previous report in which human *topors* was mapped to the chromosome 9p21 region (Chu *et al.*, 2001).

h-topors has been shown to associate with PML nuclear bodies in exponentially growing HeLa cells (Rasheed *et al.*, 2002). To examine the subcellular localization of mouse topors in mammalian cultured cells, we constructed an expression vector encoding myc-epitope-tagged topors (myc-topors) and confirmed its expression by *in vitro* transcription/translation experiments as well as transient transfection into COS-7 cells (Figure 1c and d). Consistent with the previous observation, myc-topors migrated more slowly (195 kDa) than predicted based on the calculated molecular mass, which has been suggested to be due to the phosphorylation of serine residues in the RS domain (Haluska *et al.*, 1999). The subcellular localization of myc-topors was also examined in U2-OS cells by transient overexpression. In interphase nuclei of morphologically intact transfectants, the myc-topors protein was always localized in the nuclei. Two types of transfectants were reproducibly observed. One type exhibited a fine speckled distribution to form 10–20 foci and the other type showed larger, closely spaced dots with much stronger fluorescence in the nucleoplasm but excluded from the nucleolus (data not shown). These findings were identical to those of Haluska *et al.* (1999), who described the subcellular localization of a GFP fusion with h-topors in HeLa cells.

topors interacts with p53 and enhances p53-dependent transcription in mammalian cultured cells

The putative p53-binding domains revealed by yeast two-hybrid interaction (Zhou *et al.*, 1999; Weger *et al.*,

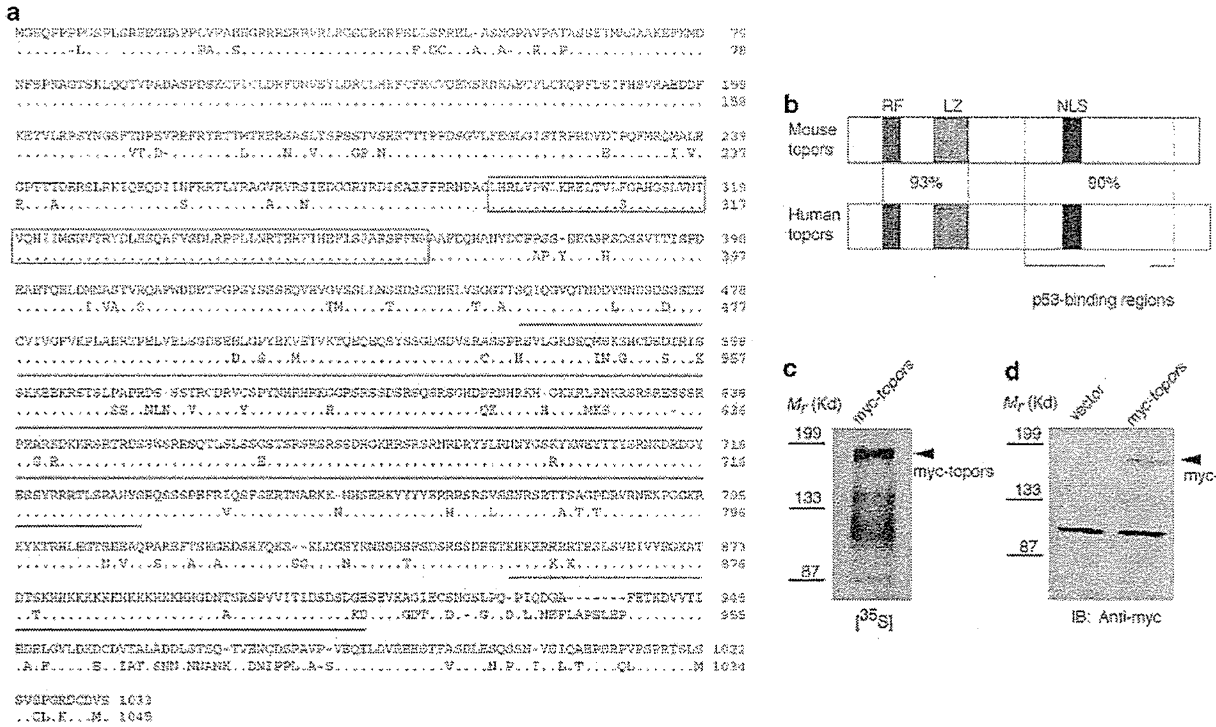

Figure 1 Amino-acid sequence, putative domain structure and expression of murine topors protein. (**a**) The deduced amino-acid sequence of mouse topors protein along with the sequence of the human counterpart. The sequences of mouse (top) and human (bottom) topors were aligned to provide the highest homology. Identical amino-acid residues are shown as dots in the human sequence; gaps are indicated by bars. Amino-acid residues in the putative RING finger motif and bipartite NLS are shown in red and blue letters, respectively. The region of the putative LZ structure is boxed with the hydrophobic residues at the first position of the heptad repeat shown in green letters. Two separate regions encoding putative p53-binding domains are underlined in red (see text). (**b**) Schematic representation of homologous domain structure shared between mouse and human topors. The RING finger motif (RF), LZ and bipartite NLS are indicated by red, green and blue boxes, respectively. Identical amino acids in each region are shown. (**c**) The myc-*topors* gene product generated by *in vitro* transcription/translation and analysed as described in Materials and methods. Relative molecular weight is indicated. (**d**) The myc-topors protein transiently overexpressed in COS-7 cells. Whole-cell lysates prepared from COS-7 cells transfected with either empty pcDNA3 (Vector, left) or pcDNA3-myc-*topors* (myc-*topors*, right) were subjected to immunoblotting analysis using the anti-myc monoclonal antibody

2002) are highly conserved between human and mouse topors (Figure 1a and b). This prompted us to examine whether myc-topors could interact with p53 in mammalian cultured cells. COS-7 cells were transiently transfected with myc-topors, and whole-cell extracts of the transfectants were subjected to immunoprecipitation with anti-p53 or normal mouse serum (NMS). As shown in Figure 2a, the anti-p53, but not the NMS, immunoprecipitates contained significant amounts of myc-topors, indicating that overexpressed myc-topors could associate with endogenous p53. This finding is consistent with the previous yeast two-hybrid studies demonstrating topors–p53 interaction (Zhou *et al.*, 1999; Weger *et al.*, 2002). We next addressed whether the physical interaction of topors with p53 might affect the function of p53. To this end, we examined the effects of overexpressed myc-topors on the p53-dependent transcription of *Bax*, *p21*^{Waf1} and *MDM2* promoters using luciferase assays in transiently transfected p53-deficient SAOS-2 and H1299 cells (Barak *et al.*, 1993; el-Deiry *et al.*, 1993; Miyashita and Reed, 1995). As shown in Figure 2b, the overexpression of myc-topors in SAOS-2 cells significantly enhanced p53-dependent transcription of the *Bax* and *MDM2* promoters in a dose-dependent manner. While myc-topors enhanced the p53-dependent activity of the *p21*^{Waf1} promoter in SAOS-2 cells, this effect did not achieve statistical significance (Figure 2b, middle panel). Similar results were obtained in H1299 cells, except that its effect on all three p53-responsive promoters was statistically significant as compared with p53 alone (Figure 2c). Under our experimental conditions, myc-topors alone had no effects on the *Bax*, *p21*^{Waf1} or *MDM2* promoter activity. We further studied whether the overexpression of topors influenced the expression of endogenous p53-regulated transcripts by quantitative real-time RT–PCR analysis of human *p21*^{Waf1} mRNA levels. As shown in Figure 2d and e, forced expression of topors enhanced the transcription of the p53 downstream gene *p21*^{Waf1} in both human small cell lung cancer SBC3 cells and U2-OS cells. Taken together, the results indicate that overexpression of topors enhances the sequence-specific transcriptional activity of p53 in a p53-dependent manner.

topors suppresses cell growth in a p53-dependent manner

These observations prompted us to investigate further whether the overexpression of myc-topors influences the growth suppression mediated by p53. For this purpose, we performed a colony formation assay using H1299 cells (lacking endogenous p53) and U2-OS cells containing the wild-type *p53* allele. The overexpression of myc-topors did not affect colony number in H1299 cells, while the colony number was significantly reduced in a dose-dependent manner in U2-OS cells (Figure 3a and b). The forced expression of p53 significantly reduced the colony number in H1299 cells, and this p53-dependent reduction was further intensified by cotransfection of pcDNA3-myc-*topors* (Figure 3a). Thus, the overexpression of topors appears to enhance the p53-dependent growth suppression of tumor cells.

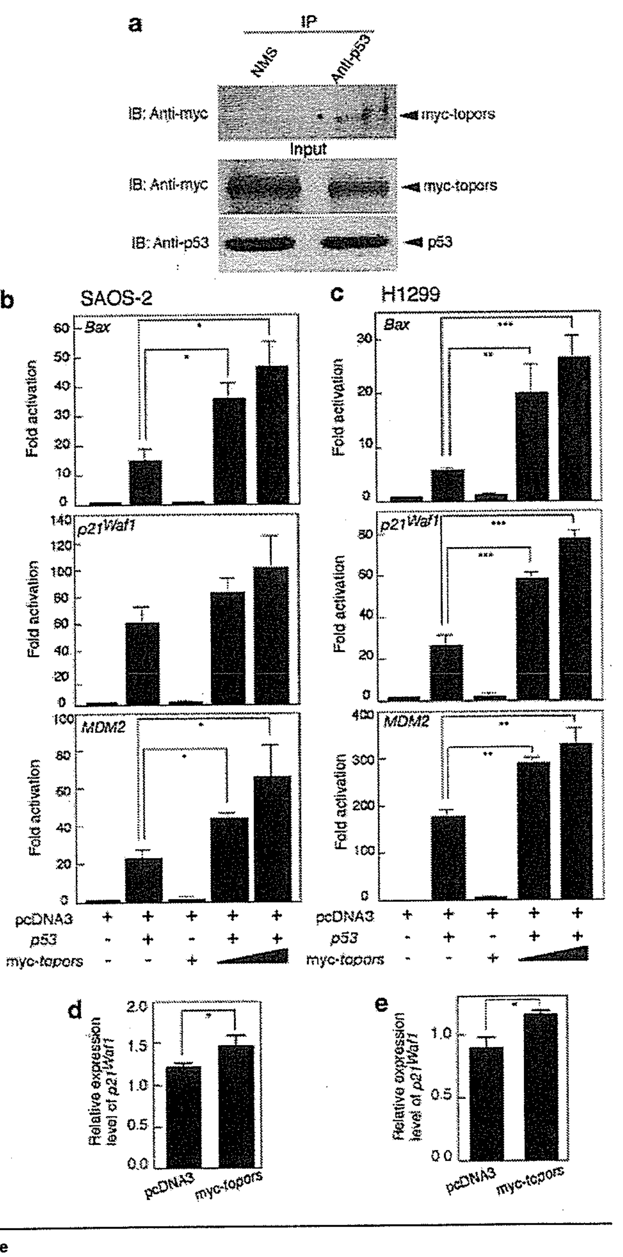

Figure 2 topors associates with p53 and activates p53-dependent transcription. (**a**) Association of transiently overexpressed myc-topors with endogenous p53 is shown by immunoprecipitation and subsequent immunoblotting analysis. (top) Whole-cell extract of COS-7 cells transfected with pcDNA3-myc-*topors* was subjected to immunoprecipitation with either NMS (left) or anti-p53 monoclonal antibodies (right) followed by immunoblotting with anti-myc monoclonal antibody. (middle and bottom) Unfractionated whole-cell extract of COS-7 cells transfected with myc-*topors* was subjected to immunoblotting using anti-myc monoclonal antibody (middle) or anti-p53 monoclonal antibody (bottom). (**b, c**) p53-deficient SAOS-2 (**b**) and H1299 (**c**) cells were transiently cotransfected with the expression plasmid for p53 along with luciferase reporter constructs containing the *Bax* (top), $p21^{Waf1}$ (middle) or *MDM2* (bottom) promoters in the presence or absence of increasing amounts of transfected pcDNA3-myc-*topors*. Transfection efficiency was standardized against *Renilla* luciferase. The average relative luciferase activities in triplicate experiments are represented as bars. Results are shown as fold induction of the luciferase activity compared with cells transfected with pcDNA3. Data shown are representative of two or three independent experiments with similar results. The significance of the differences was evaluated by Student's *t*-test (***$P<0.001$; **$P<0.01$; *$P<0.05$). (**d, e**) The expression of $p21^{Waf1}$ is upregulated by overexpression of myc-topors in small cell lung cancer cell SBC3 (**d**) and U2-OS cells (**e**). The expression of human $p21^{Waf1}$ was determined by quantitative real-time RT–PCR analysis as described in Materials and methods. Relative expression levels of $p21^{Waf1}$ were normalized to the levels of *β-actin* mRNA. The data shown are representative of two independent experiments with similar results. The significance of the differences was evaluated by Student's *t*-test (*$P<0.05$)

In different systems, p53 can induce apoptosis or cause cell cycle arrest (Ko and Prives, 1996; Vogelstein *et al.*, 2000). Because topors was able to enhance p53-dependent growth suppression, we next examined whether topors-dependent growth suppression involves apoptosis. The number of apoptotic cells exhibiting nuclear condensation and fragmentation was counted 48 h after transfection with either pcDNA3-myc-*topors* or pEGFP (Figure 3c-I–III). The number of apoptotic cells increased significantly among U2-OS cells overexpressing myc-topors compared to pEGFP transfectants (Figure 3c-IV). Thus, the growth suppression resulting from overexpression of topors may result in part from induction of apoptosis.

Since p53 activation is known to cause not only apoptosis but also cell cycle arrest, we next examined the impact of overexpressed myc-topors on cell cycle progression. For this purpose, we established stable cell lines overexpressing myc-topors. U2-OS cells were transfected with pcDNA3-myc-*topors*, and G418-resistant clones were individually isolated and screened for myc-topors expression by immunofluorescent staining. Two cell lines out of 200 clones screened were found to express myc-topors (*topors* sta-1 and *topors* sta-2), and *topors* sta-1 expressed myc-topors at a higher level than *topors* sta-2 (Figure 4a). In both of the stable transfectants, myc-topors exhibited a speckled nuclear distribution to form 10–20 foci (Figure 4b), as did endogenous mouse topors in NIH 3T3 fibroblasts (data not shown) and as reported for endogenous human topors (Rasheed *et al.*, 2002). *topors* sta-1 and *topors* sta-2 cells displayed a significantly slower growth rate

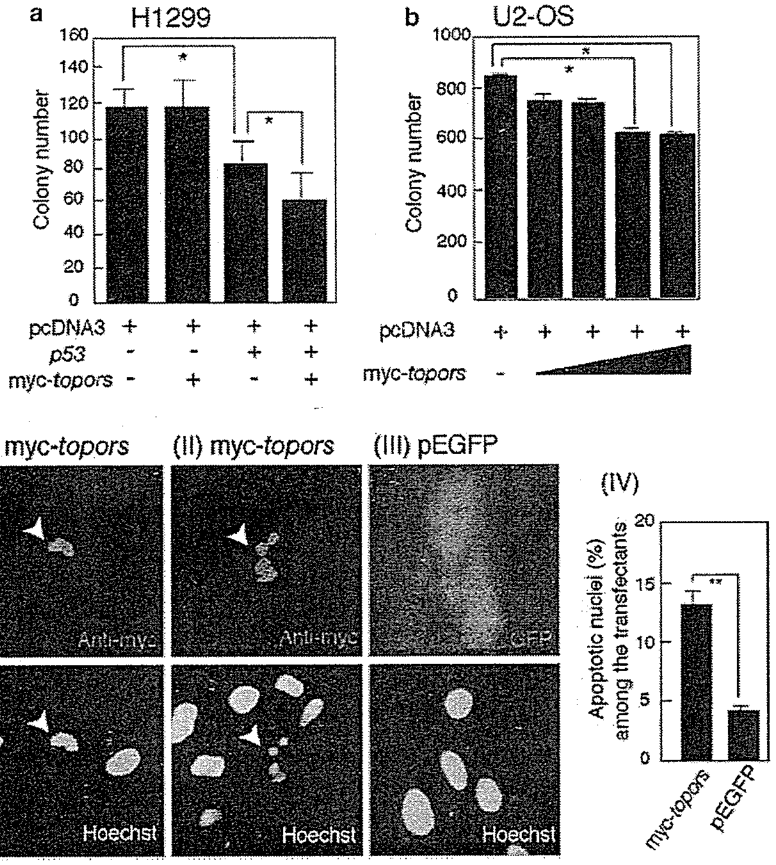

Figure 3 Enhancement of p53-dependent growth suppression and induction of apoptosis by the overexpression of topors. (**a**) The reduction in colony number by the transient overexpression of p53 is significantly enhanced by myc-topors in p53-deficient H1299 cells. (**b**) Increasing amounts of transfected myc-topors correlate with the reduction in colony number of U2-OS cells containing wild-type p53. Bars show the average numbers of colonies in triplicate experiments. The data shown are representative of three independent experiments with similar results. The significance of differences was evaluated by Student's *t*-test (*$P<0.05$). (**c**) Overexpression of myc-topors in U2-OS cells results in an increase in the number of apoptotic cells. U2-OS cells were transfected with either pcDNA3-myc-*topors* or pEGFP and transfected cells were identified by immunofluorescence staining with anti-myc monoclonal antibody or GFP expression, respectively (upper panels). Nuclear morphology was analysed after counterstaining with 1 μM Hoechst (lower panels). Cells overexpressing myc-topors frequently exhibit condensation (I) or fragmentation (II) of the nuclei, while GFP expression shows normal morphology (III). The percentages of apoptotic cells among >200 myc-topors- or GFP-positive cells were determined (IV). Values represent the means of three independent experiments. The significance of the differences was evaluated by Student's *t*-test (**$P<0.01$)

compared with the parental U2-OS cells and U2-OS cells transfected with empty vector (V-1) (Figure 4c). Of note, *topors* sta-1 cells grew more slowly than *topors* sta-2 cells, suggesting that the growth rate correlated inversely with the level of myc-topors expression in the respective cell lines. Next, asynchronous cultures of these transfectants and the parental cells were collected at 48 h after culture and their cell cycle distribution was analysed by flow cytometry. As shown in Figure 4d (cisplatin (−)) and e, *topors* sta-1 and *topors* sta-2 cells displayed a significant increase in the percentage of cells in G1 phase as compared with U2-OS and V-1 cells. A slight but reproducible increase in the sub-G1 fraction was seen exclusively in *topors* sta-1 cells (even without cisplatin treatment; see below), suggesting the constitutive occurrence of apoptosis in the *topors* sta-1 transfectants (Figure 4d and f (cisplatin (−))). The severe growth retardation of U2-OS cells stably expressing myc-topors might therefore result from both a prolonged G1 phase and a subtle induction of apoptosis. Comparison of the *topors* sta-1 and *topors* sta-2 results suggests that overexpression of topors can result in growth arrest and/or apoptosis depending on the degree of topors expression and the particular cellular context.

Stabilization of p53 by overexpression of topors

To determine whether the growth retardation produced by the stable overexpression of myc-topors was linked to the activation of p53, we next examined the expression of p53 and its response gene product, p21^{Waf1} (Harper *et al.*, 1993), in permanent transfectants. p53 was more abundantly expressed in both *topors* sta-1 and *topors* sta-2 stable transfectants than in control cell lines and the expression of p21^{Waf1} was greater in both topors

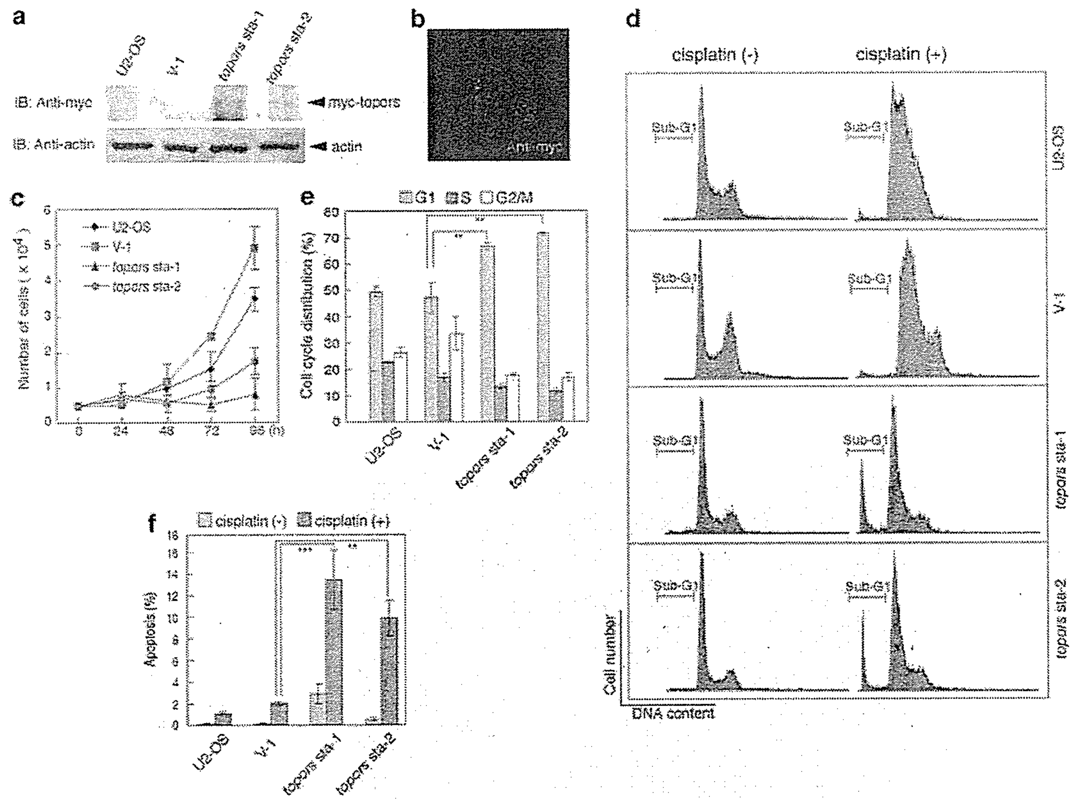

Figure 4 Cell cycle arrest and DNA damage-mediated apoptosis in U2-OS cells stably overexpressing myc-topors. (**a**) The expression of myc-topors in parental U2-OS cells and stable empty pcDNA3 vector (V-1) and pcDNA3-myc-*topors* (*topors* sta-1 and sta-2) transfectants as revealed by immunoblotting analysis using a polyclonal anti-myc antibody. The expression of actin is shown below as a loading control. (**b**) The expression pattern of myc-topors in *topors* sta-1 cell nuclei as revealed by immunofluorescent staining with anti-myc monoclonal antibody. (**c**) Growth rates of the indicated cells. The indicated cells were seeded at a density of 0.5×10^4 cells/well (12-well plate) and cell numbers were determined 1, 2, 3 and 4 days later. Average cell numbers at each time point determined in triplicate experiments are shown; standard deviations are shown in parentheses. Representative results of three independent experiments are shown. (**d**) Exponentially growing stable transfectants and control cells treated without or with cisplatin were stained with propidium iodide (PI) and subjected to FACS analysis. Representative FACS profiles of each cell line without (left) or with (right) cisplatin treatment are shown. Sub-G1 fractions are indicated. (**e**) Cell cycle profiles of exponentially growing U2-OS-derived cells as revealed by FACS analysis are shown by histograms. (**f**) Frequency of apoptotic cells among cells treated without (−) and with (+) cisplatin is shown by histograms. Values are the average percentages from triplicate experiments, and standard deviations are shown in parentheses. The experiments were repeated three times with essentially similar results. The significance of differences was evaluated by Student's *t*-test (***$P<0.001$; **$P<0.01$)

stable transfectants than in controls (Figure 5a). The increased level of p21^{Waf1} protein correlated with the topors-enhanced expression of *p21^{Waf1}* mRNA in small cell lung cancer cells and U2-OS cells shown above (Figure 2d and e). Importantly, the upregulation of p53 and p21^{Waf1} proteins in *topors* sta-1 was stronger than in *topors* sta-2, consistent with the relative expression level of ectopic myc-topors and the severity of the growth phenotypes in the two cell lines. The levels of expression of the p53 protein could also be increased by transient overexpression of myc-topors in U2-OS cells and p53-deficient large cell lung carcinoma H1299 cells, which were cotransfected with both FLAG-tagged *p53* and myc-*topors* (Figure 5c and d). Since the level of *p53* transcript was not significantly different in either of the permanent transfectants compared to controls (Figure 5b), it is likely that the increase in the amount of p53 protein was due to its stabilization. To investigate whether an increased protein half-life contributed to the elevated levels of p53 observed, we then determined the decay rate of p53 protein without and with topors overexpression. At 24 h after culture of the empty vector stable cells (V-1) and *topors* sta-2 cells, or 24 h post-transient transfection of p53-deficient human large cell lung carcinoma H1299 cells with FLAG-*p53* along with either pcDNA3 or pcDNA3-myc-*topors*, cells were treated with the protein synthesis inhibitor cycloheximide at a final concentration of 100 μg/ml for 0, 2, 4 and 6 h. The expression of p53 was then examined by immunoblotting for each time point and normalized by reference to the level of actin in each sample. As shown in Figure 5e, the p53 protein possessed a greater half-life in *topors* sta-2 cells compared with V-1 vector-transfected U2-OS cells. Similarly, the half-life of p53 was prolonged in the presence of topors compared to that of p53 cotransfected with pcDNA3 vector in p53-deficient

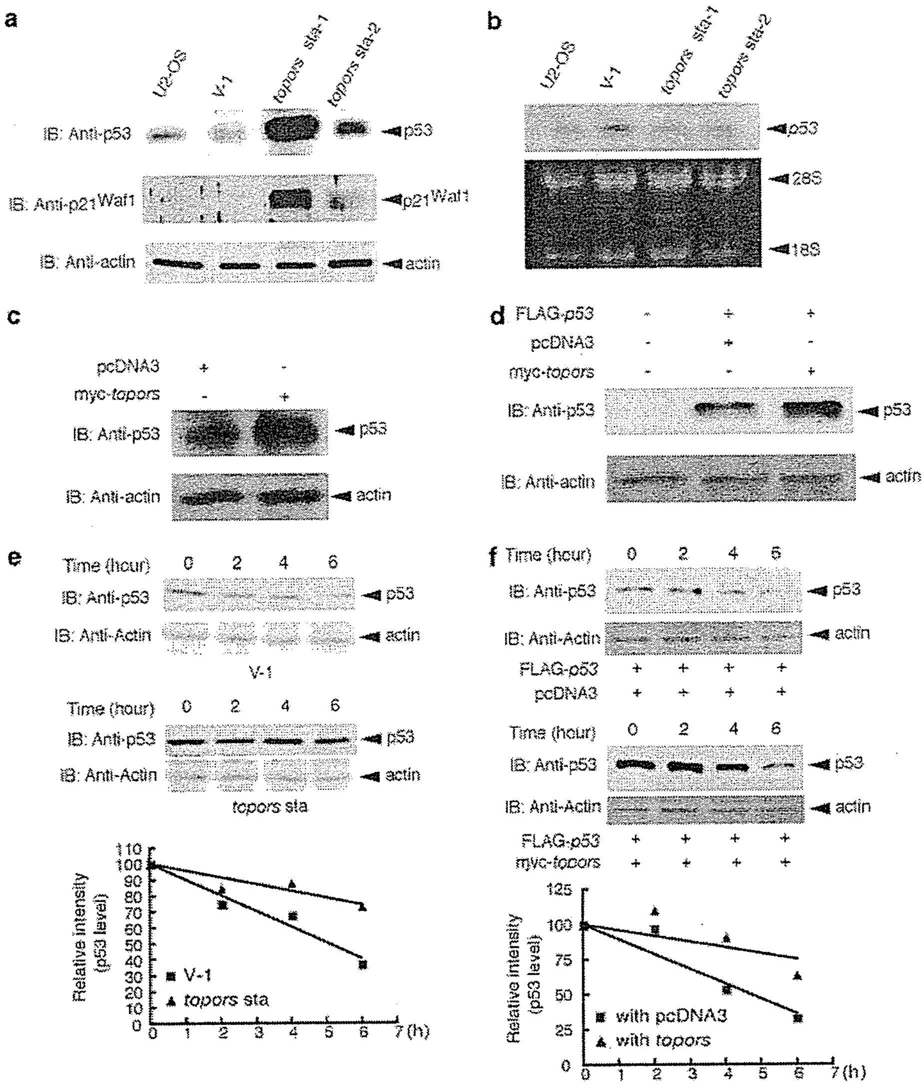

Figure 5 Stabilization of p53 protein by overexpression of myc-topors. (**a**) The expressions of p53 and p21^{Waf1} in parental U2-OS cells and stable transfectants of pcDNA3 vector (V-1) and pcDNA3-myc-*topors* (*topors* sta-1 and sta-2) as revealed by immunoblotting analysis. The expression of actin is shown as a loading control. (**b**) The expression of *p53* transcript in each cell line as revealed by RNA blot analysis (upper panel). Ethidium bromide staining of 28S and 18S ribosomal RNA is shown as a loading control (lower panel). (**c**) The expression of p53 in U2-OS cells after transfection with pcDNA3 or pcDNA3-myc-*topors*. The expression of actin is shown as a loading control. (**d**) The expression of p53 in H1299 cells after transfection without or with FLAG-*p53* in the presence of pcDNA3 or pcDNA3-myc-*topors*. The expression of actin is shown as a loading control. (**e, f**) Increase in the half-life of p53 by topors. At 24 h after culture of pcDNA3 stable cells (V-1) and *topors* sta-2 cells (**e**), or at 24 h after transient transfection of p53-deficient H1299 cells (**f**) with expression plasmid of FLAG-*p53* along with pcDNA3 or pcDNA3-myc-*topors*, cycloheximide was added to the culture medium and the cells were extracted at the indicated time points. Whole-cell lysates were subjected to immunoblotting. The relative intensities of p53 were quantified by densitometric scanning, which normalized to actin, and are represented graphically

H1299 cells (Figure 5f). Taken together, these data suggest that expression of topors increases p53 levels by stabilizing p53 protein and thereby enhancing its ability to limit cell growth.

topors expression is induced by DNA damage

Our finding that transient or stable transfection of topors upregulates p53 levels suggests that topors could be a rate-limiting factor in the regulation of p53 function. If this is the case, a quantitative alteration of topors expression in a given cell could affect its apoptotic response to genotoxic reagents. To address this possibility, exponentially growing U2-OS cells or stable transfectants were treated with 20 μM cisplatin for 24 h, and the cells were then subjected to the cell cycle analysis. Following cisplatin treatment, both *topors* sta-1 and *topors* sta-2 cells demonstrated significantly increased sub-G1 fractions compared to the control cells (Figure 4d and f). The fraction of apoptotic cells among the *topors* sta-1 and *topors* sta-2 transfectants reached 80–90% after 48 h of cisplatin treatment, compared to only 30–40% in control cells (data not shown). Thus, the overexpression of topors enhances the apoptotic response of U2-OS cells to DNA damage.

This finding suggests that upregulation of endogenous topors might be involved in mediating p53-dependent cellular responses to stress stimuli. We thus examined the expression of endogenous *topors* after cisplatin treatment in U2-OS cells. *topors* expression was obviously upregulated 24 and 48 h after cisplatin treatment consistent with the expression of p53 protein (Figure 6a). The analysis was extended to primary MEFs and C-20 cells, a mouse cell line derived from colon carcinoma. In these cells before treatment, *topors* was constitutively expressed while p53 was barely detectable. The apoptotic response of MEFs and C-20 cells to 20 μM cisplatin was more prominent than that of U2-OS cells (Figure 6b and c; compare to Figure 4d). The expression of the *topors* gene and p53 protein was increased in MEFs and C-20 cells by cisplatin treatment as well (Figure 6b and c). Since topors is a topoisomerase I-binding protein, we further investigated whether the expression of *topors* is also induced after treatment by CPT, a potent antineoplastic inhibitor of topoisomerase I (Haluska *et al.*, 1999). As shown in Figure 6d, when U2-OS cells and NIH 3T3 cells were treated with CPT at the concentration of 10 μM, the expression of *topors* increased more than twofold compared to cells without treatment. However, it is still possible that the upregulation of *topors* mRNA might be a consequence of p53 induced during DNA damage-induced apoptosis. To exclude this possibility, we examined *topors* expression after overexpression of p53 by transient transfection. The overexpression of p53 did not significantly affect *topors* transcript levels (Figure 6e). Taken together, the induction of *topors* by the genotoxic reagents provides a mechanism to facilitate the p53-mediated DNA damage-dependent apoptosis in tumor and primary cells.

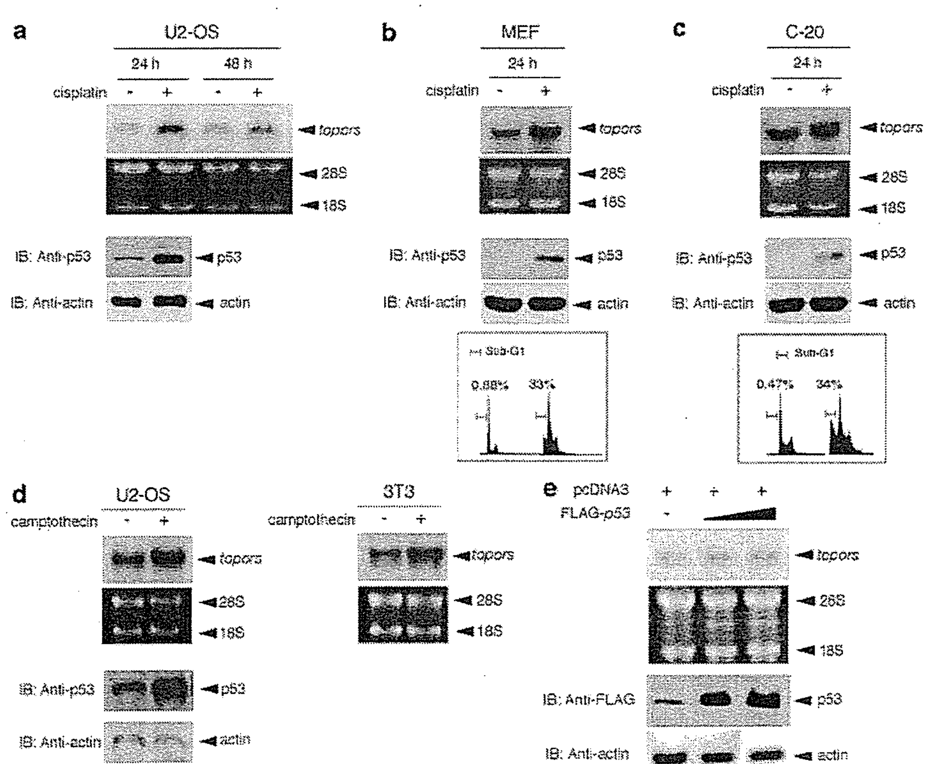

Figure 6 Induction of endogenous *topors* expression by DNA damage in human and mouse cell lines. (**a**) The expressions of *topors* and p53 are significantly induced in U2-OS cells in response to cisplatin treatment as revealed by RNA blot and immunoblotting analysis, respectively. (upper panels) *topors* transcripts detected as 4.0-kb bands (top) and ethidium bromide staining of 28S and 18S ribosomal as a loading control are shown (bottom). (lower panels) The expressions of p53 (top) and actin (lower) as a loading control are shown. (**b, c**) Induction of *topors* (upper panels), p53 expression (middle panels) and FACS analysis-based estimation of apoptosis (lower panels) by cisplatin treatment are also seen in primary MEFs (**b**) and murine colon carcinoma cells (C-20) (**c**). Percentages of cells in the sub-G1 fraction are shown in the lower panels. (**d**) The expressions of *topors* and p53 are significantly induced in U2-OS cells and NIH/3T3 cells in response to 12-h CPT treatment as revealed by Northern blot and immunoblotting, respectively. (upper panels) *topors* transcripts (top) and ethidium bromide staining of 28S and 18S ribosomal as a loading control are shown (bottom). (lower panel) The expressions of p53 (top) and actin (lower) as a loading control in U2-OS cells are shown. (**e**) The expression of *topors* is not affected by the transient overexpression of p53 in U2-OS cells. Increasing amounts of FLAG-*p53* documented by immunoblotting analysis (lower panels) do not significantly affect the expression of endogenous *topors* (upper panels). Ethidium bromide staining of 28S and 18S ribosomal RNA is shown as a loading control

Discussion

In the present study, we identify the mouse counterpart of human topors and document its involvement in p53-regulated cell growth control. Overexpressed topors associates with p53, activates p53-dependent transcription via the stabilization of p53 and, consequently, induces either cell cycle arrest or apoptosis in a dose-dependent manner. Therefore, our observations strongly implicate the topors protein as a novel coactivator of the p53 tumor suppressor protein.

We further show that expression of endogenous *topors*, as well as the p53 protein, is induced by DNA damage in tumor and primary cells. The present observations indicate that topors mediates p53-dependent cellular responses to some forms of DNA damage and, thus, could act as a tumor suppressor that activates p53. Interestingly, the human *topors* gene maps to chromosome 9p21 where the tumor suppressor genes associated with 86% of small cell lung carcinomas are suggested to reside and the above observations provide further evidence for the *topors* gene as a candidate tumor suppressor gene mapped to this region. Our preliminary studies have revealed that *topors* mRNA is expressed in all small cell lung cancer cell lines at levels similar to other tumor cell lines (L Lin and A Hata, unpublished data). Most recently, Oyanagi *et al.* (2004) revealed that the expression of *LUN* (*topors*) gene is downregulated in the development and metastases of lung cancer, suggesting that *LUN* might play important roles in inhibiting the oncogenesis of non-small cell lung cancer. The expression of topors protein in normal lung tissues and small cell lung cancers will require further future study.

The data clearly show that the overexpression of topors may cause either cell cycle arrest or apoptosis, and suggest that which occurs depends both on the topors level and the cellular context, although other variables require further exploration. There is a positive correlation between the amount of p53 protein and overexpressed topors in U2-OS cells in both transient and stable transfectants. Since it has repeatedly been reported that low levels of p53 expression are antiapoptotic while high levels promote apoptosis, high levels of topors could facilitate apoptosis due to the high level of p53 expression (Chen *et al.*, 1996; Lassus *et al.*, 1996). This phenomenon is further supported by another observation made in this study. We identified only two stable transfectants overexpressing myc-topors from 200 G418-resistant colonies and both exhibited a lower level of topors expression than that seen in the transiently transfected cells. This implies that only U2-OS cells overexpressing permissive amounts of exogenous topors might be allowed to survive by escaping apoptotic outbursts and instead exhibiting G1 cell cycle arrest, which is correlated with the induction of the downstream gene of p53, *p21^{Waf1}*. Interestingly, slight but significant apoptotic outbursts coincide with G1 arrest in *topors* sta-1, but not sta-2, cells. Slightly higher expression levels of myc-topors and, consequently, p53 in *topors* sta-1 cells than in sta-2 cells may be the cause for this phenotypical difference.

Our findings demonstrate that the expression level of topors protein may be a rate-limiting factor in the regulation of p53 activity. While this manuscript was in preparation, Saleem *et al.* (2004) also reported that transient expression of h-topors showed antiproliferative activity and was associated with G0/G1 cell cycle arrest in HeLa cells. Our results additionally show that overexpression of topors could activate the expression of p53 and induce either cell cycle arrest or apoptotic response.

In this study, we show that endogenous topors is significantly upregulated by the genotoxic reagents at the level of transcription in tumor and primary cells. A previous study has suggested that post-translational regulation of topors by DNA damage may also be involved (Rasheed *et al.*, 2002). In that study, overexpressed GFP-topors fusion protein immediately relocalized from PML nuclear bodies to the nucleoplasm in cells exposed to CPT or DRB. Since DRB exposure has also been shown to induce the accumulation of diffuse p53 in the nucleoplasm, it is possible that the relocalization of topors into the nucleoplasm might allow its association with and subsequent stabilization of p53 (Klibanov *et al.*, 2001).

The stability of the tumor suppressor p53 is crucial for its function to induce cell cycle arrest and/or apoptosis as a consequence of its ability to bind to specific DNA sequences and activate the transcription of adjacent genes (Vogelstein *et al.*, 2000). Overexpression of topors increased the stability of p53 and correspondingly enhanced the p53-dependent transcriptional activities. topors contains a RING finger motif, a domain that has been implicated in protein–DNA and protein–protein interactions, E2-dependent ubiquitination and SUMO conjugation (Kahyo *et al.*, 2001; Matthews and Sunde, 2002). Indeed, topors proteins have been recently shown to possess evolutionarily conserved E3 ubiquitin ligase activity. A *Drosophila* topors was shown to mediate Hairy polyubiquitination, resulting in Hairy, but not Dmp53 or topoisomerase I (dTopoI), degradation (Secombe and Parkhurst, 2004). Human GFP-topors fusion protein was shown to function as an E3 ligase for p53, albeit to a lesser degree than MDM2 (Rajendra *et al.*, 2004). Therefore, topors could affect the stability of p53 via covalent modification of p53 by ubiquitin isopeptide. This observation, however, is not necessarily consistent with our and others' previous observations suggesting topors as a likely tumor suppressor protein since polyubiquitination of p53 mediated by GFP-topors induces proteasome-dependent downregulation of p53 in U2-OS cells (Chu *et al.*, 2001; Rajendra *et al.*, 2004; Saleem *et al.*, 2004). This implies that regulation of p53 by topors may involve not only ubiquitination but also some other molecular mechanism.

Recently, the activity of p53 has been reported to be positively regulated by SUMO conjugation, which is mediated, at least in part, by another RING finger protein, PIAS (Gostissa *et al.*, 1999; Rodriguez *et al.*, 1999; Kahyo *et al.*, 2001). Sequence similarity between two regions of topors and human PIASx protein, the RING domains and putative SUMO-1 interaction motifs suggests the possibility that topors may function as a SUMO E3 ligase (Weger *et al.*, 2003). Indeed, h-topors and several components of SUMO-conjugating systems have been isolated together as interacting proteins with Mx1, an interferon-inducible GTPase that is associated with PML nuclear bodies (Engelhardt *et al.*, 2001), which include p53, pRb, DAXX and CBP (Mann and Miller, 2004). Thus, topors may contribute to p53 stabilization or activation via SUMO conjugation processes.

The molecular mechanisms underlying the stabilization and/or activation of p53 by topors may also involve protein–protein interactions. AAV-2 Rep78/68 has been shown to possess a tumor suppressor property and to bind physically to p53 to prevent the adenovirus-mediated degradation of p53 (Batchu *et al.*, 1999). Since topors is capable of interacting not only with p53, but also with Rep78/68, topors may cooperate with Rep78/68 to stabilize p53. It is possible that endogenous cellular regulators of p53 may function in ways analogous to these viral products and cooperate with topors to stabilize p53. These possibilities are not necessarily mutually exclusive. It will be essential to address experimentally the possible catalytic activities of topors.

Materials and methods

Isolation and preparation of an expression vector for a full-length cDNA of topors

Yeast two-hybrid screening was performed to isolate the cDNAs for Mph2-binding proteins from a cDNA library derived from E11.0 mouse embryo as described previously, and 177 independent clones were found to be positive for β-galactosidase activities as examined by filter assay (Vojtek *et al.*, 1993; Kingma and Osheroff, 1998; Yamaki *et al.*, 2002). The nucleotide sequences of the positive cDNA clones were determined. Two clones contained 1.2-kb cDNA fragments that were highly homologous to *h-topors* (Haluska *et al.*, 1999). To isolate a full-length *topors* cDNA, a radiolabeled 1.2-kb cDNA fragment was used as a probe to screen the mouse brain cDNA library. After three rounds of hybridization, six positive clones were obtained and their nucleotide sequences were determined. The longest cDNA, containing a 3.5-kb insert, turned out to encode from the RING finger motif to the stop codon, but lacked a putative *topors* initiation codon. By searching public databases of mouse ESTs, we found a cDNA clone (MNCb-6014) that overlapped with the 3.5-kb cDNA clone. MNCb-6014, which was kindly provided by Dr Katsuyuki Hashimoto (Division of Genetic Resources, National Institute of Infectious Diseases, Japan), contained a *topors* initiation codon, but instead lacked the carboxyl-terminal region. To generate an expression vector encoding a full-length *topors*, the 5′-region of MNCb-6014 was amplified with primers 5′-CGTCGACAAGCTTATGGGGTCGCAGCCGCC-3′ (the *Sal*I/*Hind*III restriction sites are underlined) and 5′-CAGAAGACAGTTCAACAAGTTCCGGGGTCC-3′ using the MNCb-6014 cDNA clone as a template. The PCR product was digested with *Sal*I and *Sph*I and subcloned into the identical restriction sites of the above-mentioned plasmid containing the 3.5-kb insert to produce a full-length cDNA for *topors* (pBluscript-M-*topors*). The pBluscript-M-*topors* was digested with *Hind*III and *Not*I and introduced into the identical restriction sites of pcDNA3-myc (Invitrogen, Carlsbad, CA, USA) to generate an expression vector for myc-tagged topors (pcDNA3-myc-*topors*).

In vitro *transcription/translation of the topors gene product*

The topors protein was generated from the pcDNA3-myc-*topors* vector using the T7-TNT Quick-Coupled Transcription–Translation system (Promega, Madison, WI, USA) in the presence of [^{35}S]methionine (Amersham Biosciences Inc., Piscataway, NJ, USA) according to the manufacturer's instructions. The quality of the synthesized protein was verified by electrophoresis though an 8% SDS–polyacrylamide gel and autoradiography.

Cell culture and transfection

Human osteosarcoma cell lines U2-OS and SAOS-2, COS-7, NIH/3T3 and primary MEFs were maintained in DMEM supplemented with 10% FBS and antibiotics. Human large cell lung carcinoma H1299 cells and human small cell lung cancer SBC3 cells were grown in RPMI-1640 medium supplemented with 10% FBS and antibiotics. All cells were cultured at 37°C in a water-saturated atmosphere of 5% CO_2 in air. COS-7 and U2-OS cells contain wild-type p53, while SAOS-2 and H1299 cells are deficient in p53 expression. For transfection, U2-OS cells were transfected by either the calcium phosphate co-precipitation method or Lipofectamine 2000 transfection reagent (Invitrogen, Grand Island, NY, USA) in accordance with the manufacturer's specifications. COS-7 cells were transfected with the FuGENE6 transfection reagent (Roche Molecular Biochemicals, Indianapolis, IN, USA). H1299 and SAOS-2 cells were transfected with the LipofectAMINE Plus transfection kit (Invitrogen, Grand Island, NY, USA) according to the manufacturer's protocol. To obtain stable transfectants, either pcDNA3 or pcDNA3-myc-*topors* was introduced into the exponentially growing U2-OS cells by the calcium phosphate co-precipitation method. At 48 h post-transfection, the cells were transferred to fresh medium containing G418 at a final concentration of 800 μg/ml. At 1 week after selection, drug-resistant colonies were isolated and the expression of myc-topors was examined by immunofluorescence staining as described below. As a control, a stable cell line of the pcDNA3 vector was established.

Immunoprecipitation and immunoblotting

Transfected cells were washed in ice-cold phosphate-buffered saline (PBS), lysed in lysis buffer (25 mM Tris-Cl, pH 7.5, 137 mM NaCl, 2.7 mM KCl, 1% Triton X-100 and 1 mM PMSF) and the extracts were sonicated briefly and centrifuged at 800 *g* for 5 min to remove insoluble materials. The protein concentrations were determined by the Bradford protein assay (Bio-Rad, Hercules, CA, USA) using BSA as a standard. For immunoprecipitation, the cell lysates prepared from COS-7 cells transfected with pcDNA3-myc-*topors* were precleared using protein G-Sepharose beads at 4°C for 30 min under gentle rotation, and then incubated with either NMS or antibodies against p53 (DO-1, Oncogene Research Products, Cambridge, MA, USA and Pab1801, Santa Cruz Biotechnology Inc., Santa Cruz, CA, USA) at 4°C for 2 h. The immune complexes were then recovered with protein G-Sepharose beads. The immunoprecipitates or supernatants were subjected to SDS–polyacrylamide gel electrophoresis and electrophoretically transferred onto Immobilon P membranes (Millipore

Corp., Bedford, MA, USA). The membranes were blocked with TBS containing 0.1% Tween 20 and 5% nonfat dry milk, probed with antibodies against c-myc epitope (562, Medical and Biological Laboratories, Nagoya, Japan), p53 (DO-1, Oncogene Research Products, Cambridge, MA, USA), *p21*^{Waf1} (H-164, Santa Cruz), *β*-actin (20-33, Sigma Chemical Co., St Louis, MO, USA) and FLAG (M2, Sigma Chemical Co., St Louis, MO, USA), and then incubated with horse radish peroxidase-conjugated goat anti-rabbit or anti-mouse secondary antibody (Santa Cruz Biotechnology Inc., Santa Cruz, CA, USA). Immunoreactive bands were visualized with an ECL Western blot detection kit (Amersham Biosciences Inc., Piscataway, NJ, USA).

Immunofluorescence and confocal microscopy

Transfected cells grown on coverslips were fixed with 3.7% formaldehyde for 30 min at room temperature, permeabilized with 0.2% Triton X-100 for 5 min at room temperature and then incubated with 3% BSA in PBS for 2 h to reduce nonspecific antibody binding. Immunostaining was performed by incubating cells with a monoclonal anti-myc antibody (9E10, diluted 1:10) for 1 h at room temperature in a humidified chamber, followed by incubation with fluorescein isothiocyanate (FITC)-conjugated goat anti-mouse IgG (diluted 1:250) for 1 h at room temperature. The coverslips were washed extensively with PBS, mounted with PermaFluor (Immunon, Pittsburgh, PA, USA) and the labeled cells were examined using a confocal laser scan microscope (LSM510; Carl Zeiss Co., Ltd, Jena, Germany).

Luciferase reporter assay

SAOS-2 or H1299 cells were seeded at a density of 5×10^4 cells/well in a 12-well tissue culture dish and then cotransfected with 100 ng of p53/p73-responsive luciferase reporter constructs carrying *Bax*, *p21*^{Waf1} or *MDM2* promoter, 10 ng of pRL-TK and 25 ng of the p53 expression plasmid in either the presence or absence of increasing amounts of pcDNA3-myc-*topors* as described previously (Watanabe *et al.*, 2002). The total amounts of DNA used in each transfection were kept constant (510 ng/transfection) using pcDNA3. Luciferase assays were performed 48 h post-transfection with a dual luciferase reporter assay system (Promega) according to the manufacturer's instructions.

Quantitative real-time RT–PCR analysis

Small cell lung cancer cell SBC3 and U2-OS cells were transfected with pcDNA3 or myc-*topors*. At 48 h after transfection, total RNA was extracted with the RNeasy Mini kit (Qiagen Inc., Valencia, CA, USA). Quantitative real-time RT–PCR was performed using the Brilliant SYBR Green QRT-PCR Master Mix Kit, 1-Step (Stratagene, La Jolla, CA, USA) and specific primers for human *p21*^{Waf1} and human *β-actin*. Quantitative results of *p21*^{Waf1} mRNA were normalized for the levels of *β-actin* mRNA. Specific primers for *p21*^{Waf1} are as follows: 5′-ATGAAATTCACCCCCTTTCC-3′ (forward primer) and 5′-CCCTAGGCTGTGCTCACTTC-3′ (reverse primer).

Colony formation assay

U2-OS and H1299 cells were transfected with pcDNA3 or pcDNA3-myc-*topors* in the presence or absence of FLAG-*p53* (a kind gift from Dr Toshiharu Suzuki, University of Tokyo, Tokyo, Japan). After 48 h of culture, the cells were divided into new dishes and cultured for 2 weeks in the presence of 400 μg/ml of G418. The cell dishes were fixed, stained with Giemsa's solution (Merck KgaA, 54271, Darmstadt, Germany, Art. 1.09204) and the colonies were counted.

Analyses of cell cycle and apoptosis

After treating cells with or without cisplatin (Sigma Chemical Co., St Louis, MO, USA) at a final concentration of 20 μM for 24 h, both floating and adherent cells were collected by brief centrifugation, fixed in 70% (v/v) ethanol for more than 4 h at −20°C and stained with PI (Sigma Chemical Co., St Louis, MO, USA). To identify cells with sub-G1 DNA content, the fluorescence of the nuclei was measured by flow cytometry (FACScan, Becton Dickinson, Oxford, UK). At least 5×10^4 events were analysed with Cell Quest software. For the morphological assessment of fragmented nuclei, U2-OS cells grown on coverslips were transfected with either myc-*topors* or pEGFP-N3 (BD Biosciences, CA, USA). At 48 h post-transfection, the cells were fixed with 3.7% formaldehyde, permeabilized with 0.2% Triton X-100 and blocked with 3% BSA in PBS. myc-topors was visualized with 9E10 monoclonal antibody (diluted 1:10) followed by FITC-conjugated goat anti-mouse IgG (diluted 1:250). DNA was visualized by incubating the cells with 1 mM Hoechst 33258 dye. Cells showing apoptotic morphological changes were analysed under a Leica QFluoro confocal spectral microscope (Leica Microsystems Imaging Solutions Ltd, Cambridge, UK).

Protein half-life determination

At 24 h after culture of the pcDNA3 stable cells (V-1) and *topors* sta-2 cells, or at 24 h post-transfection of p53-deficient human H1299 cells with FLAG-*p53* in combination with either pcDNA3 or pcDNA3-myc-*topors*, cycloheximide (Sigma) was added to the cell culture medium at a final concentration of 100 μg/ml. Cells were collected at the indicated time points and whole-cell extracts were subjected to immunoblot analysis with anti-p53 antibody. Best-fit linear regression analysis of the data points was performed with Prism 4.0 software (GraphPad).

Northern blot analysis

U2-OS cells, MEFs, C-20 cells and NIH/3T3 cells were cultured in the presence of cisplatin (20 μM) for 24 or 48 h or CPT (10 μM) for 12 h. Total cellular RNA was isolated using the Isogen kit (Wako Pure Chemical Industries, Ltd, Osaka, Japan). RNA (10 μg) was denatured in formaldehyde-formamide, separated by electrophoresis in 1.5% agarose gels and transferred to Hybond™-N+ membranes (Amersham Biosciences, Tokyo, Japan). The resulting blots were individually hybridized with radiolabeled probes specific for *topors* and *p53* at 65°C for more than 10 h. The filters were washed twice with 2 × SSC (300 mM NaCl and 30 mM sodium citrate, pH 7.0)/0.1% *N*-lauroyl sarcosine at room temperature for 30 min, and then once with 1 × SSC/0.1% *N*-lauroyl sarcosine at 55°C for 30 min.

Statistical analysis

Statistical analyses were performed using the unpaired Student's *t*-test. The differences between two groups were considered to be statistically significant when $P < 0.05$.

Acknowledgements
We are grateful to Dr M Vidal and Dr O Tetsu for critical reading of the manuscript, Dr O Ohara for providing the mouse cDNA library, Dr T Oda for providing the pBTM116

vector, Ms Sanae Takeda, Dr Jie Liu and Dr Tomomi Kaneko for kind assistance and Dr T Akasaka for initial instructions on yeast two-hybrid screening. This project was supported by a grant-in-aid for Scientific Research on Priority Areas and for Scientific Research (B) and Special Coordination Funds for Promoting Science and Technology from the Ministry of Education, Culture, Sports, Science and Technology of the Japanese Government to HK and AN.

References

Barak Y, Juven T, Haffner R and Oren M. (1993). *EMBO J.*, **12,** 461–468.
Batchu RB, Shammas MA, Wang JY and Munshi NC. (1999). *Cancer Res.*, **59,** 3592–3595.
Chen X, Ko LJ, Jayaraman L and Prives C. (1996). *Genes Dev.*, **10,** 2438–2451.
Chu D, Kakazu N, Gorrin-Rivas MJ, Lu HP, Kawata M, Abe T, Ueda K and Adachi Y. (2001). *J. Biol. Chem.*, **276,** 14004–14013.
el-Deiry WS, Tokino T, Velculescu VE, Levy DB, Parsons R, Trent JM, Lin D, Mercer WE, Kinzler KW and Vogelstein B. (1993). *Cell*, **75,** 817–825.
Engelhardt OG, Ullrich E, Kochs G and Haller O. (2001). *Exp. Cell Res.*, **271,** 286–295.
Gostissa M, Hengstermann A, Fogal V, Sandy P, Schwarz SE, Scheffner M and Del Sal G. (1999). *EMBO J.*, **18,** 6462–6471.
Haluska Jr P, Saleem A, Rasheed Z, Ahmed F, Su EW, Liu LF and Rubin EH. (1999). *Nucleic Acids Res.*, **27,** 2538–2544.
Harper JW, Adami GR, Wei N, Keyomarsi K and Elledge SJ. (1993). *Cell*, **75,** 805–816.
Kahyo T, Nishida T and Yasuda H. (2001). *Mol. Cell*, **8,** 713–718.
Kingma PS and Osheroff N. (1998). *Biochim. Biophys. Acta*, **1400,** 223–232.
Klibanov SA, O'Hagan HM and Ljungman M. (2001). *J. Cell Sci.*, **114,** 1867–1873.
Ko LJ and Prives C. (1996). *Genes Dev.*, **10,** 1054–1072.
Lane DP. (1992). *Nature*, **358,** 15–16.
Lassus P, Ferlin M, Piette J and Hibner U. (1996). *EMBO J.*, **15,** 4566–4573.
Levine AJ. (1997). *Cell*, **88,** 323–331.
Mann KK and Miller Jr WH. (2004). *Cancer Cell*, **5,** 307–309.
Matthews JM and Sunde M. (2002). *IUBMB Life*, **54,** 351–355.
Miyashita T and Reed JC. (1995). *Cell*, **80,** 293–299.
Oyanagi H, Takenaka K, Ishikawa S, Kawano Y, Adachi Y, Ueda K, Wada H and Tanaka F. (2004). *Lung Cancer*, **46,** 21–28.
Rajendra R, Malegaonkar D, Pungaliya P, Marshall H, Rasheed Z, Brownell J, Liu LF, Lutzker S, Saleem A and Rubin EH. (2004). *J. Biol. Chem.*, **279,** 36440–36444.
Rasheed ZA, Saleem A, Ravee Y, Pandolfi PP and Rubin EH. (2002). *Exp. Cell Res.*, **277,** 152–160.
Rodriguez MS, Desterro JM, Lain S, Midgley CA, Lane DP and Hay RT. (1999). *EMBO J.*, **18,** 6455–6461.
Saleem A, Dutta J, Malegaonkar D, Rasheed F, Rasheed Z, Rajendra R, Marshall H, Luo M, Li H and Rubin EH. (2004). *Oncogene*, **23,** 5293–5300.
Schlehofer JR. (1994). *Mutat. Res.*, **305,** 303–313.
Secombe J and Parkhurst SM. (2004). *J. Biol. Chem.*, **279,** 17126–17133.
Sionov RV and Haupt Y. (1999). *Oncogene*, **18,** 6145–6157.
Vogelstein B, Lane D and Levine AJ. (2000). *Nature*, **408,** 307–310.
Vojtek AB, Hollenberg SM and Cooper JA. (1993). *Cell*, **74,** 205–214.
Watanabe K, Ozaki T, Nakagawa T, Miyazaki K, Takahashi M, Hosoda M, Hayashi S, Todo S and Nakagawara A. (2002). *J. Biol. Chem.*, **277,** 15113–15123.
Weger S, Hammer E and Engstler M. (2003). *Exp. Cell Res.*, **290,** 13–27.
Weger S, Hammer E and Heilbronn R. (2002). *J. Gen. Virol.*, **83,** 511–516.
Yamaki M, Isono K, Takada Y, Abe K, Akasaka T, Tanzawa H and Koseki H. (2002). *Gene*, **288,** 103–110.
Zhou R, Wen H and Ao SZ. (1999). *Gene*, **235,** 93–101.

Oncogene (2005) 24, 938–944
© 2005 Nature Publishing Group All rights reserved 0950-9232/05 $30.00
www.nature.com/onc

Protein stability and function of p73 are modulated by a physical interaction with RanBPM in mammalian cultured cells

Sonja Kramer[1], Toshinori Ozaki[1], Kou Miyazaki[1], Chiaki Kato[1], Takayuki Hanamoto[1] and Akira Nakagawara*,[1]

[1]*Division of Biochemistry, Chiba Cancer Center Research Institute, 666-2 Nitona, Chuoh-ku, Chiba 260-8717, Japan*

Upon a certain DNA damage including cisplatin treatment, p73 is stabilized and exerts its growth-suppressive and/or proapoptotic function. However, the precise molecular basis by which the intracellular levels of p73 are regulated remains unclear. In the present study, we have identified RanBPM as a novel binding partner of p73α by yeast-based two-hybrid screening, and also found that RanBPM has an ability to stabilize p73α. GST pull-down assays and co-immunoprecipitation experiments revealed that RanBPM directly bound to the extreme COOH-terminal region of p73α, whereas it failed to interact with p53. Co-expression of RanBPM with p73α resulted in the nuclear translocation of RanBPM, and both proteins co-localized in cell nucleus as examined by indirect immunofluorescent staining. It is worth noting that the expression of RanBPM inhibited the ubiquitination of p73α, and thereby prolonged its half-life. Subsequent studies demonstrated that the proapoptotic activity of p73α was significantly enhanced in the presence of RanBPM. Taken together, our present findings implicate a novel role for RanBPM in the regulation of p73 stability and function.
Oncogene (2005) **24,** 938–944. doi:10.1038/sj.onc.1208257
Published online 22 November 2004

Keywords: p53; p73; RanBPM; two-hybrid; ubiquitination

p73 is a newly identified p53-related nuclear transcription factor, and functions to promote cell cycle arrest and/or apoptosis (Kaghad *et al.*, 1997). These cellular roles of p73 are largely attributed to its ability to transactivate specific target genes. In contrast to p53, p73 is expressed as multiple isoforms arising from either alternative splicing or alternative promoter usage (Melino *et al.*, 2002). Although functional differences among the splicing isoforms with different COOH-termini remain unclear, NH_2-terminally truncated forms of p73 (ΔNp73) have an oncogenic potential and exhibit a dominant-negative behavior toward wild-type p73 as well as p53 (Pozniak *et al.*, 2000; Nakagawa *et al.*, 2002; Stiewe *et al.*, 2002).

Steady-state levels of p73 are kept extremely low under normal conditions, however, p73 is significantly induced at protein level in response to a certain genotoxic stress including cisplatin treatment, which is mediated by a nuclear nonreceptor tyrosine kinase c-Abl (Agami *et al.*, 1999; Gong *et al.*, 1999; Yuan *et al.*, 1999). c-Abl binds to the PXXP motif of p73 and phosphorylates p73 at Tyr-99. Alternatively, Ren *et al.* (2002) reported that protein kinase Cδ catalytic fragment phosphorylates p73 at Ser-289, and increases its stability, suggesting that post-translational modification such as phosphorylation might contribute to increase the stability of p73. Protein phosphorylation has been shown to be involved in the initiation of protein ubiquitination by E3 ubiquitin ligase (Carrano *et al.*, 1999; Ganoth *et al.*, 2001). As described previously (Balint *et al.*, 1999; Lee and La Thangue, 1999), p73 is regulated at least in part by the protein degradation process through the ubiquitin–proteasome system. Additionally, Lee and La Thangue (1999) described that the COOH-terminal region of p73α might have a regulatory role in the proteasome-dependent degradation of p73. Recently, we have found that MM1 and RACK1 interact with the extreme COOH-terminal region of p73α, and regulate its transcriptional activity as well as proapoptotic function (Watanabe *et al.*, 2002; Ozaki *et al.*, 2003). However, these interactions did not have a detectable effect on the intracellular levels of p73α.

To identify the possible cellular protein(s) involved in the regulation of p73 protein stability, we screened a cDNA library derived from human fetal brain using the extreme COOH-terminal region of p73α (amino-acid residues 551–636) as a bait in a yeast-based two-hybrid system. After screening of approximately 5×10^5 transformants, 12 independent clones exhibited a high level of β-galactosidase activity, and subsequent sequence analysis revealed that three out of them encoded the overlapping regions of RanBPM (Figure 1a). RanBPM was initially identified as a cellular protein that can interact with Ran nuclear–cytoplasmic transport protein (Nakamura *et al.*, 1998; Nishitani *et al.*, 2001), and contained the putative SPRY domain which might be involved in protein–protein interactions (Ponting *et al.*, 1997). Although most of the Ran-binding proteins play an important role in nucleocytoplasmic transport, it is

*Correspondence: A Nakagawara;
E-mail: akiranak@chiba-ccri.chuo.chiba.jp
Received 16 July 2004; revised 4 October 2004; accepted 6 October 2004; published online 22 November 2004

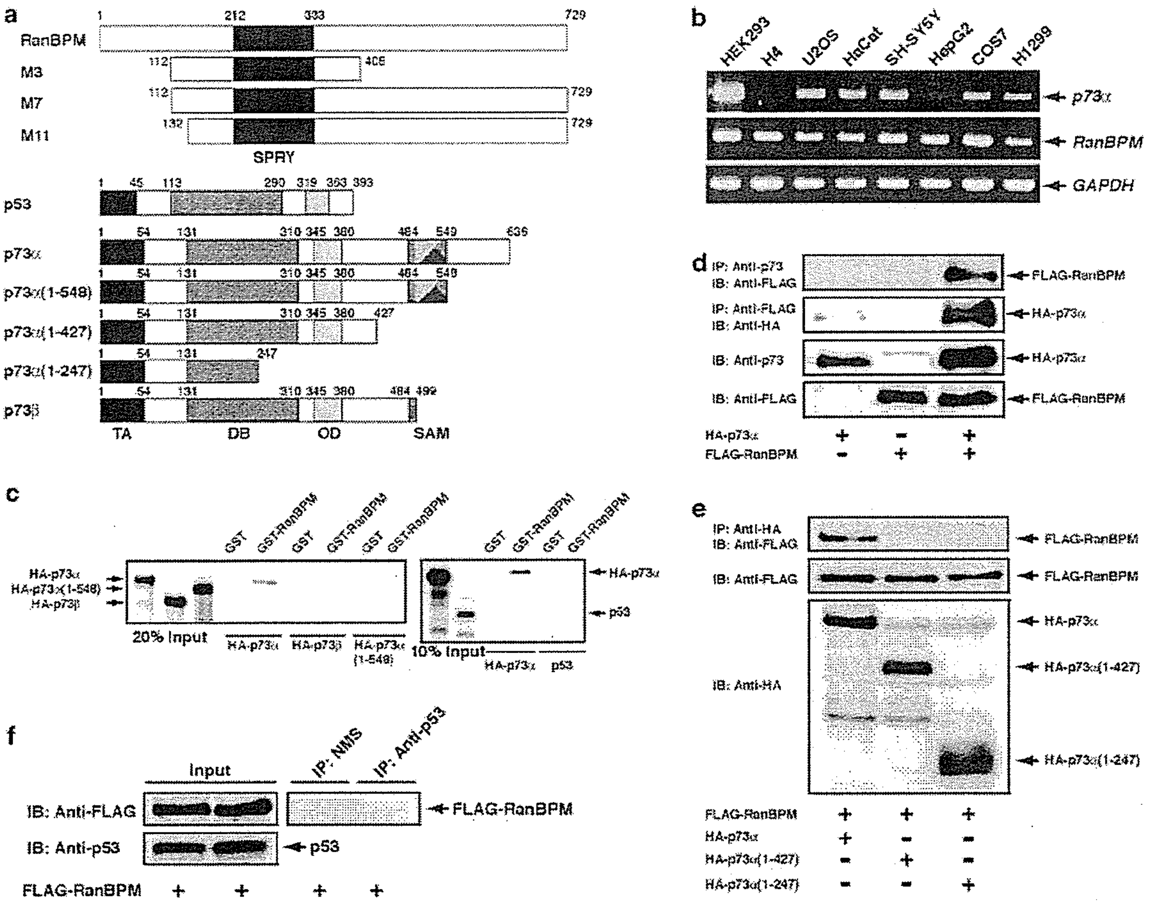

Figure 1 Identification of RanBPM as a binding partner of p73. (**a**) The three overlapping RanBPM clones (M3, M7 and M11) isolated from the yeast two-hybrid screening along with the full-length RanBPM are shown. The putative SPRY domain (amino-acid residues 212–333) is indicated. Structures of p73 and p53 are also shown. TA, transactivation domain; DB, DNA-binding domain; OD, oligomerization domain; SAM, sterile α motif domain. Amino-acid numbering was relative to first methionine, which represents position +1. (**b**) Expression of *RanBPM* and *p73*. Total RNA prepared from the indicated cell lines were incubated with SuperScript II reverse transcriptase (Invitrogen, Carlsbad, CA, USA), and generated cDNAs were amplified by PCR in the presence of primers specific for *p73* (top panel), *RanBPM* (middle panel) or *GAPDH* (bottom panel). (**c**) GST pull-down assay. *In vitro* translated ^{35}S-labeled p73α, p73β, p73α (1–548) or p53 was incubated with bacterially expressed GST or GST-RanBPM(112–408) for 2 h at 4°C. Bound complexes were recovered on the glutathione–sepharose beads (Amersham Pharmacia Biotech, Piscataway, NJ, USA), washed extensively with the binding buffer (50 mM Tris–HCl, pH 7.5, 150 mM NaCl, 0.1% Nonidet P-40, 1 mM EDTA, and 1 mM phenylmethylsulfonyl fluoride), and then boiled in SDS sample buffer. Bound proteins were resolved by 10% SDS–polyacrylamide gel, and analysed by autoradiography. The input of the radio-labeled proteins used in the binding reaction is also shown. (**d**) p73α interacts with RanBPM in mammalian cultured cells. COS7 cells transfected with the indicated expression plasmids were lysed in 25 mM Tris–HCl, pH 8.0, 137 mM NaCl, 1% Triton X-100 and 1 mM phenylmethylsulfonyl fluoride. Whole-cell lysates were immunoprecipitated with anti-p73 antibody (Ab-4, NeoMarkers, Fremont, CA, USA) or anti-FLAG (M2, Sigma, St Louis, MO, USA), and subjected to immunoblotting with anti-FLAG (first panel) or with anti-HA (12CA5, Roche Molecular Biochemicals, Indianapolis, IN, USA) antibody (second panel), respectively. Separate aliquots of the lysates were immunoblotted with anti-p73 (third panel) or anti-FLAG antibody (fourth panel) to confirm the expression of FLAG-RanBPM or HA-p73α, respectively. (**e**) COOH-terminal region of p73α is required for the interaction with RanBPM. COS7 cells were co-transfected with the indicated combinations of the expression plasmids, and whole-cell lysates were immunoprecipitated with anti-HA antibody, followed by immunoblotting with anti-FLAG antibody (top panel). Cell lysates were immunoblotted as a control for FLAG-RanBPM (middle panel), HA-p73α and HA-p73α derivatives (bottom panel) in the input lysate. (**f**) p53 does not bind to RanBPM. Cell lysates prepared from COS7 cells transfected with FLAG-RanBPM were immunoprecipitated with the normal mouse serum (NMS, Jackson ImmunoResearch Laboratories, West Grove, PA, USA) or anti-p53 antibodies (DO-1 plus PAb1801, Oncogene Research Products, Cambridge, MA, USA). Immunoprecipitates were analysed by immunoblotting with anti-FLAG antibody (right panel). Left panels show the Western blotting with anti-FLAG, or anti-p53 antibody to monitor the expression level of FLAG-RanBPM or the endogenous p53, respectively

unlikely that RanBPM is involved in this process (Nishitani *et al.*, 2001). Alternatively, Nakamura *et al.* (1998) reported that RanBPM might be involved in reorganization of the microtubule network; however, the precise function of RanBPM remains unknown. Consistent with the previous observations (Rao *et al.*, 2002), *RanBPM* was expressed in various cell lines (Figure 1b). To confirm the interaction between RanBPM and p73, we performed GST pull-down assays using a GST fusion protein containing RanBPM